AD-A035 867 NAVAL ELECTRONICS LAB CENTER SAN DIEGO CALIF F/G 20/6
FIBER OPTICS AND INTEGRATED OPTICS TECHNIQUES FOR SIGNAL PROCES--ETC(U)
FEB 77 G M DILLARD, B R HUNT, H F TAYLOR

UNCLASSIFIED NELC/TR-2013 NL

1 OF 1
ADA035867

END

DATE
FILMED
3-77

NELC / TR 2013

[redacted]

NELC / TR 2013

AD A035867

(12)

FIBER OPTICS AND INTEGRATED OPTICS TECHNIQUES FOR SIGNAL PROCESSING

George M Dillard, Barry R Hunt, and Henry F Taylor 1 February 1977

Research and Development, April to September 1976

Prepared for
NAVAL ELECTRONIC SYSTEMS COMMAND

[redacted]

NAVAL ELECTRONICS LABORATORY CENTER
SAN DIEGO, CALIFORNIA 92152

UNCLASSIFIED

SECURITY CLASSIFICATION OF THIS PAGE (When Data Entered)

REPORT DOCUMENTATION PAGE

READ INSTRUCTIONS BEFORE COMPLETING FORM

1. REPORT NUMBER: NELC Technical Report 2013 (TR 2013)
2. GOVT ACCESSION NO.
3. RECIPIENT'S CATALOG NUMBER

4. TITLE (and Subtitle): FIBER OPTICS AND INTEGRATED OPTICS TECHNIQUES FOR SIGNAL PROCESSING

5. TYPE OF REPORT & PERIOD COVERED: Research and Development rept. April — September 1976

6. PERFORMING ORG. REPORT NUMBER

7. AUTHOR(s): George M. Dillard, Barry R. Hunt, Henry F. Taylor

8. CONTRACT OR GRANT NUMBER(s)

9. PERFORMING ORGANIZATION NAME AND ADDRESS: Naval Electronics Laboratory Center, San Diego, California 92152

10. PROGRAM ELEMENT, PROJECT, TASK AREA & WORK UNIT NUMBERS: 62762N, F54583, XF54583005, NELC F225

11. CONTROLLING OFFICE NAME AND ADDRESS: Naval Electronic Systems Command, Support Technology Division, Washington, DC 20360

12. REPORT DATE: 1 February 1977

13. NUMBER OF PAGES: 68

14. MONITORING AGENCY NAME & ADDRESS (if different from Controlling Office): NELC/TR-2013

15. SECURITY CLASS. (of this report): Unclassified

15a. DECLASSIFICATION/DOWNGRADING SCHEDULE

16. DISTRIBUTION STATEMENT (of this Report): Approved for public release; distribution is unlimited. F54583

17. DISTRIBUTION STATEMENT (of the abstract entered in Block 20, if different from Report)

18. SUPPLEMENTARY NOTES

19. KEY WORDS (Continue on reverse side if necessary and identify by block number)

Optical circuits	Radar systems	Pseudorandom coding
Integrated optics	Electronic warfare	
Fiber optics	Analog-to-digital conversion	
Signal processing	Transversal filters	

20. ABSTRACT (Continue on reverse side if necessary and identify by block number)

This report introduces some new device concepts based on the technologies of fiber optics and integrated optics, and discusses the potential uses of these devices in signal processing. Analog-to-digital converters, delay-line devices (including transversal filters), pseudorandom sequence generators, rf spectrum analyzers, and switching networks are described and analyzed in some detail. Applications for these devices in the improvement of signal processing for radar, electronic warfare, communications, and multisensor data collection systems are investigated. It is concluded that the new optical technologies offer →

DD FORM 1 JAN 73 1473 EDITION OF 1 NOV 65 IS OBSOLETE

UNCLASSIFIED

SECURITY CLASSIFICATION OF THIS PAGE (When Data Entered)

403 940

LB

20. *Continued*

the potential for substantial reduction in size, weight, and power and improvement in performance and/or cost over present or alternative techniques for a variety of systems which process broadband (greater than 100-MHz bandwidth) signals.

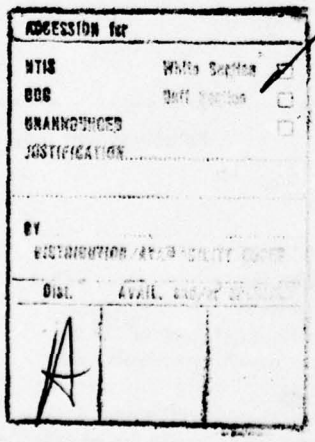

OBJECTIVES

Investigate and develop new device concepts based on the technologies of fiber optics and integrated optics, with particular emphasis on the application of these devices in signal processing. Analyze analog-to-digital converters, delay-line devices (including transversal filters), pseudorandom sequence generators, rf spectrum analyzers, and switching networks. Investigate applications for these devices in signal processing for radar, electronic warfare, communications, and multisensor data collection systems.

RESULTS

1. The technologies of fiber optics and integrated optics have developed rapidly, enabling the development of low-loss fibers, long-life injection lasers, high-capacity, high-gain optical repeaters, fast-response optical modulator-switches, multichannel optical switches and switching networks, and low-loss couplers for single-mode fibers and devices.

2. The potential capabilities of fiber and integrated optics techniques begin to surpass that of other information processing methods when the processing rate approaches 10^8 (100 million) operations per second. Promising devices are analog-to-digital converters, delay lines, transversal filters, pseudorandom sequence generators, Bragg cell spectrum analyzers, and switching networks.

3. Fiber and integrated optics components offer substantial improvements in the signal-processing functions required by radar systems, including matched filtering, pulse-to-pulse integration, and the generation and processing of complex waveforms.

4. Fiber and integrated optics components are potentially powerful tools for electronic warfare applications. These include signal analysis and sorting in ESM, generation of complex waveforms for active EW, accurate determination of direction of arrival for uhf and vhf signals, the realization of several unique ESM techniques with medium-range multiple receiving platforms and dedicated data links, and the high-speed digitization and recording of broadband ELINT signals.

5. Pseudorandom sequence generators utilizing fiber and integrated optics offer the possibility of generating and combining long sequences at gigachip rates, and could lead to substantial improvements in data rates, probability of intercept, or immunity from jamming in spread spectrum systems.

6. Integrated optics switches, used in conjunction with electronic central processing units, buffers, and memories, offer the possibility of substantial improvement in computation speed for multisensor correlation problems.

RECOMMENDATIONS

1. Implement an 8-beam feasibility test model of the fiber optic beam-forming antenna for ESM direction finding in the vhf/uhf band and determine the sensitivity, dynamic range, and angular accuracy.

2. Develop an eight-bit optical A/D converter operating at 1 gigaword/second with a fiber loop for recirculating data storage.

3. Use the A/D converter described in paragraph 2 to demonstrate the feasibility of signal analysis for exotic ESM waveforms and monopulse imaging for high-resolution radar.

4. Perform feasibility study, operational analysis, and cost-benefit projections of multiple-platform ESM techniques that could be implemented using fiber optics and integrated optics.

5. Develop a 1-gigabit/second optical pseudorandom sequence generator for spread-spectrum communications.

6. Develop a fiber optics recursive filter for demonstrating feasibility of pulse-to-pulse integration in high-resolution radars.

7. Investigate the effectiveness of tailored waveform generation using a programmable fiber optics transversal filter (PFOTF) for jamming and deception purposes. If warranted by the results of the investigation, develop such a waveform generator.

8. Perform systems analysis and computer simulation of hybrid Bragg cell-PFOTF superheterodyne and IFM receivers and determine if projected capabilities warrant development of such a system and associated components.

9. Demonstrate the feasibility of Bragg cell dynamic range improvement using fiber optics.

ADMINISTRATIVE INFORMATION

This work was performed under 62762N, F54583, XF 54583005 (NELC F225) by members of the EO/Optics Division and the Passive EW Division, Electromagnetic Systems Department, and the Tactical Command Control and Navigation Division, Information Systems Department, for the Naval Electronic Systems Command (ELEX 304). This report covers work performed from April to September 1976 and was approved for publication on 1 February 1977.

ACKNOWLEDGMENTS

The authors would like to express appreciation to a number of people who have contributed information and ideas during the preparation of this report. These include D Albares, J Cassaboom, W Dejka, C Erickson, P Fletcher, V Hildebrand, R Lowry, H Miller, R Perry, M Prickett, W Richards, R Shearer, B Summers, V Tenney, B Vainik, and D Wehner of NELC; R Kahn, Information Processing Techniques, Advanced Research Projects Agency; D Lewis, Office of Naval Research; D Hecht and R Corcoran of the ATI Division of ITEK; and H Mandelberg, A Rupp, P Szczepanek, and B Wooton of the National Security Agency. Appreciation is also expressed to L Strom and J Tegnelia, Tactical Technology Office, Advanced Research Projects Agency; W Sooy, Science Applications, Inc; and R Kenan and K Verber, Battelle Columbus Laboratories, who organized and led a DoD/industry workshop on the applications of integrated optics in Monterey, CA, in July 1976, and a followup session in Washington, DC, in October 1976. These meetings, attended by the authors, provided a useful forum for discussion of most of the concepts described in this document.

We would also like to acknowledge and thank Betty Snyder, Code 3300, NELC, who skillfully and quickly typed the original manuscript and retyped several revised versions.

Finally, we would like to thank N Butler and L Sumney, NAVELEX-304; N Mathis and E Maynard, NELC Technology Program Management Office; C E Bergman, Technical Director, NELC; and CAPT R Gavazzi, Commanding Officer, NELC, for helpful suggestions and encouragement during the course of this work.

CONTENTS

I. INTRODUCTION

"Integrated optics" is concerned with the development of thin-film dielectric waveguide components for carrying out a variety of operations on guided light beams. Generation of light, detection, modulation, switching, and directional coupling are potentially useful functions which have already been demonstrated in integrated optics devices.[1-3] "Circuits" made up of a number of components interconnected by waveguides on a single substrate might make possible orders-of-magnitude improvement in reliability, ruggedness, speed of operation, size, weight, electrical power requirements, and costs in electro-optics systems. The spectacular success that has been achieved in replacing discrete components with integrated circuits in the electronics industry encourages us to look forward to similar results in electro-optics. Furthermore, the present state of the relevant technologies is favorable for the development of integrated optics. Methods for producing excellent substrates, films, and high-resolution patterns are now available, so that we can be reasonably confident that most of the devices that can be designed on paper can actually be fabricated with today's technology.

Some of the functions originally suggested and more recently demonstrated in integrated optics are analogous to those performed by microwave components for metallic waveguide communication systems. Indeed, it is no accident that the recent surge of interest in thin-film optical devices began at about the same time (1969-70) that the first glass fibers with losses low enough (~20 dB/km) for long-distance telecommunications were produced in research laboratories. In recent years, considerable progress has been made in the development of components for wideband optical communication, using glass fibers as the transmission medium.[4,5] The most dramatic advance has been in the loss in the fibers themselves, which has dropped from a minimum of about 1000 dB/km prior to 1969 to less than 1 dB/km today.[6]

Most of the research and development effort to date in fiber optics and integrated optics technologies has been directed towards communications applications. Recently, it has been realized that there are also important potential uses for these technologies in military systems for the processing of wideband signals. Basic signal processing functions which can be performed using optical fibers include signal delay, matched filtering, and data storage, while integrated optics devices can be used for analog-to-digital (A/D) conversion, switching, and rf spectrum analysis, as well as for signal modulation and demodulation at the terminations of fiber delay lines. The ability to perform these functions at gigahertz rates using optical techniques could make possible dramatic performance improvements, and, in some cases, provide entirely new capabilities for real-time signal processing in a variety of military systems.

This report is intended for those in the applications community who are concerned with applying new concepts and techniques to military systems and for those in the

---

[1]Tamir, T, ed, Integrated Optics, Springer Verlag, Berlin, 1975

[2]Kogelnik, H, "An Introduction to Integrated Optics," IEEE Trans Microwave Theory and Techniques, v MTT-23, p 2-16, January 1975

[3]Taylor, HF and Yariv, A, "Guided Wave Optics," Proc IEEE, v 62, p 1044-1060, August 1974

[4]Personick, SD, "Optical Fibers, a New Transmission Medium," Communications Society, v 13, p 20-24, January 1975

[5]Miller, SE, Maractili, EAJ, and Li, T, "Research Toward Optical Fiber Transmission Systems," Proc IEEE, v 61, p 1703-1751, December 1973

[6]Horiguchi, M, and Osanai, H, "Spectral Losses of Low-OH-Content Optical Fibers," Electron Lett, v 12, p 310-312, 10 June 1976.

technology and device development communities with an interest in fiber optics and integrated optics. It summarizes the findings of a study carried out by NELC personnel to assess the potential uses of fiber optics and integrated optics techniques in signal processing for radar, electronic warfare (EW), spread spectrum communications, and undersea surveillance. In section II following this Introduction, the basic elements (sources, detectors, modulators, fibers) of the technology are described and the state-of-the-art for each is summarized. In section III the operation and characteristics of signal processing devices using fiber and integrated optics technologies are discussed and a comparison is made with alternative methods. Analog-to-digital converters, delay-line devices, pseudorandom sequence generators, rf spectrum analyzers, and switching networks are the devices or functional elements covered. Section IV is concerned with applications of these devices in the areas of radar, electronic warfare, spread spectrum communications, and multisensor correlation. In each of these areas, an assessment is made of ways in which specific types of systems could utilize the technology and the expected improvements or new capabilities. Finally, section V summarizes the findings with respect to both the technology and applications and section VI presents recommendations for future research and development directed towards realization of systems for which the technology offers a high payoff potential.

II. BASIC OPTICAL COMPONENTS

This section describes the optical sources, detectors and receivers, modulators and switches, and optical fibers which are the basic elements or building blocks for the signal processing devices described in section III.

A. OPTICAL SOURCES

A rather wide variety of optical sources can be considered for use with fiber optics and integrated optics devices. These include semiconductor light-emitting diodes (LED's) and injection lasers, helium neon gas lasers, and Nd:YAG solid-state lasers.

The technology for producing the semiconductor light sources has evolved rapidly over the past few years, in part because they are the preferred type of light emitter for use in fiber optics communications.[4,5] The LED and injection laser are both pn junction diodes which, when passing current in the forward-biased condition, emit light generated by electron-hole recombination. The laser is designed such that a resonant optical cavity is formed by parallel reflectors (generally, the cleaved surfaces of the crystal) situated on either side of the recombination region. In the LED, the emission spectrum is essentially that of the spontaneous emission of the material modified by its absorption, and typically has a spectral width of 300–500 Å. In the injection laser, the cavity resonance causes substantial narrowing of the emission spectrum to a spectral width of 50 Å or less, as well as improved directionality and phase coherence characteristic of stimulated emission. Both LED's and injection lasers have the advantages of small size, light weight, low drive voltage (~1.5 V), and relatively good power conversion efficiency (1–10%). In addition, both can be modulated by varying the drive current (direct modulation), with cutoff frequencies of several hundred megahertz for some LED's and in excess of 1 gigahertz for some lasers. Most LED's display good linearity of output power as a function of drive current, and in injection lasers the variation of power with changes in drive current is generally close to linear above the threshold current, which marks the onset of stimulated laser emission, as illustrated in fig 1.

With regard to the applications described in this report, the LED suffers the disadvantage that, since it emits incoherent light, the coupling to single-mode fibers and waveguides is very inefficient. The use of the LED in these applications therefore would be limited to the generation of optical signals for coupling into multimode fiber delay lines in cases where high time-bandwidth products are not needed. On the other hand, coupling from an injection laser to a single-mode fiber or waveguide can be quite efficient. Ideally, the injection laser will emit in a single transverse mode with the spatial distribution of the electromagnetic field closely matched to that of the fiber or waveguide mode. Substantial progress has been made in approaching this ideal in gallium-aluminum arsenide stripe-geometry injection lasers.[7,8] One example of an injection laser designed for good beam confinement in both transverse dimensions[9] is illustrated schematically in fig 2. As much as 20% of the light from a cw, room-temperature injection laser has been coupled into a single-mode

---

[7]Lee, TP, and Cho, AY, "Single-Transverse-Mode Injection Lasers with Embedded Stripe Laser Grown by Molecular Beam Epitaxy," Appl Phys Lett, v 29, p 164–166, 1 August 1976

[8]Blum, J, McGroddy, JC, McMullin, PG, Shih, KK, Smith, AW, and Ziegler, JF, "Oxygen-implanted Double-Heterojunction GaAs/GaAlAs Injection Lasers," IEEE J Quant Electron, v QE-11, p 413–418, July 1975

[9]Lee, TP, Burrus, CA, Miller, BI, and Logan, RA, "$Al_xGa_{1-x}As$ Double-Heterostructure Rib-Waveguide Injection Laser," IEEE J Quant Electron, v QE-11, p 432–435, July 1975

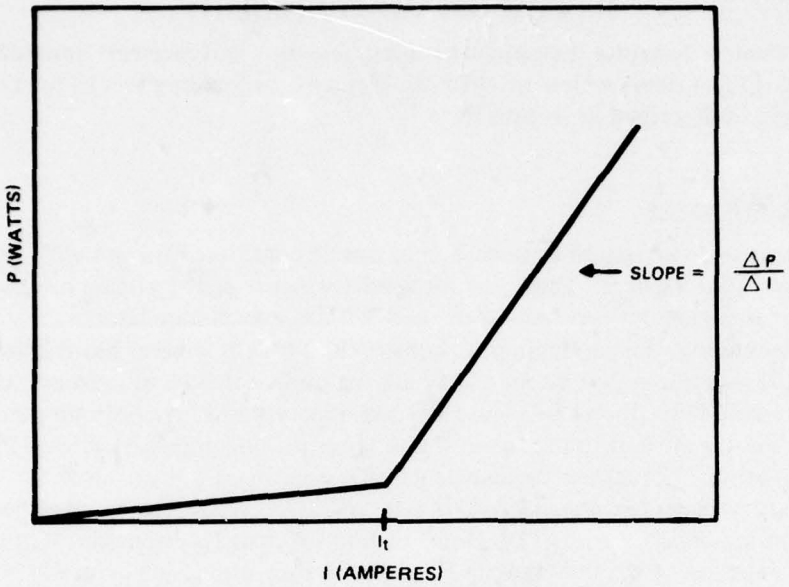

Figure 1. Idealized plot of the optical power output, P, as a function of drive current, I, for a semiconductor injection laser. The power output is approximately a linear function of current when I exceeds the threshold current, I_t, which is typically in the 100–300-mA range.

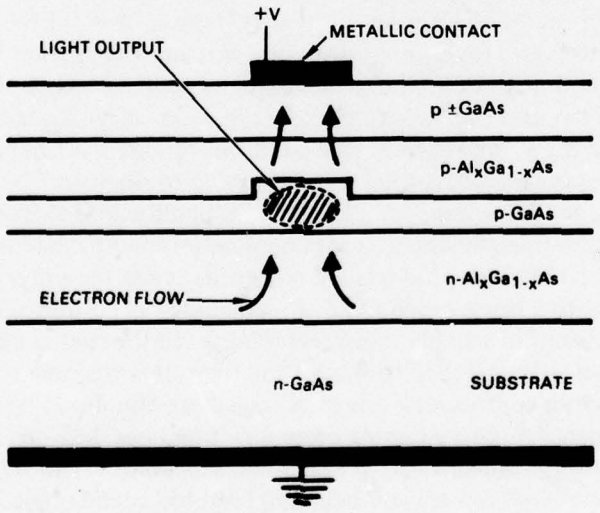

Figure 2. Schematic diagram of a $Ga_xAl_{1-x}As$ double-heterostructure injection laser designed for operation in a single transverse mode. The refractive index of the P-GaAs layer exceeds that of the adjacent layer to provide for waveguiding in the vertical direction, and the step in that layer confines the beam in the horizontal direction. The light is generated by the recombination of the injected electrons and holes in the pn junction region.

fiber,[10] and further improvements resulting from better control of the laser mode characteristics can be anticipated. Until recently, operating life for the injection lasers under cw or high-duty-cycle operation at ambient temperatures, was considered an important technological barrier. However, operating lifetimes of several thousand hours are now routinely achieved for both laboratory and commercial devices, and 10^5–10^6 hours are projected by some manufacturers.

The helium-neon (HeNe) laser has proven to be a useful tool for studying waveguide devices in the laboratory, and could be an alternative to the injection laser in some devices. Helium-neon lasers are now mass-produced for such applications as video cassette players and supermarket checkout label readers, and sell commercially for less than $100. The primary advantage over injection lasers is the superior beam quality for efficient coupling to single-mode waveguides. The shorter wavelength of the visible HeNe line (0.63 μm versus ~0.80 μm for the injection laser) would allow a reduction of approximately 20% in length or drive voltage for an electro-optic modulator or switch. However, the large size, low electrical-optical conversion efficiency (~0.001%), and the need for external modulation eliminate the HeNe laser from consideration for most of the devices described in this report.

The Nd:YAG laser is attractive for use with fiber delay lines because losses of the fibers are lower at its emission wavelength of 1.06 μm than at shorter wavelengths, so that longer fibers can be used, and because its spectral purity makes it possible to obtain very low pulse dispersion in a long fiber. It is anticipated that these characteristics will make it possible to achieve extremely high time-bandwidth products in a fiber delay line. In addition, the Nd:YAG laser can readily be mode-locked to produce short (50–100 ps) pulses. A train of these pulses as an input to an optical A/D converter would provide a natural "sampling window" to eliminate the need for an electronic sample-and-hold, which is a limiting component in the design of present electronic A/D converters. Unfortunately, present commercial flash-lamp-pumped Nd:YAG laser systems are much too expensive ($15 000) and bulky to be practical for these applications. However, the use of injection lasers or LED's to pump small Nd:YAG rods shows promise as a way to obtain a small, inexpensive 1.06-μm laser. As such lasers become available, they can be considered for use with the guided-wave devices described in this report.

B. PHOTODETECTORS AND RECEIVERS

A variety of solid-state photodetectors can be considered for use in converting the output of a guided-wave optical device to an electrical signal. Silicon PIN and avalanche photodiodes, which have been standard commercial products for a number of years, are most sensitive at near-infrared wavelengths. The silicon PIN and avalanche detectors are both operated as backbiased diodes and are designed so that as much of the incident light as possible is absorbed in a region of intrinsic silicon.[11] The photogenerated electrons and holes are swept out of the intrinsic region towards the contacts by the applied field. In the avalanche device, electrons from the intrinsic region enter a pn junction region with high electric fields in which carrier multiplication takes place, as illustrated in fig 3. The electrons and holes in this region acquire enough energy from the field to produce additional carriers by ionization,

---

[10] Pavlopoulos, TG, private communication

[11] DiDimenico, M, "A Review of Fiber Optical Transmission Systems," Optical Engineering, v 13, p 423–428, September–October 1974

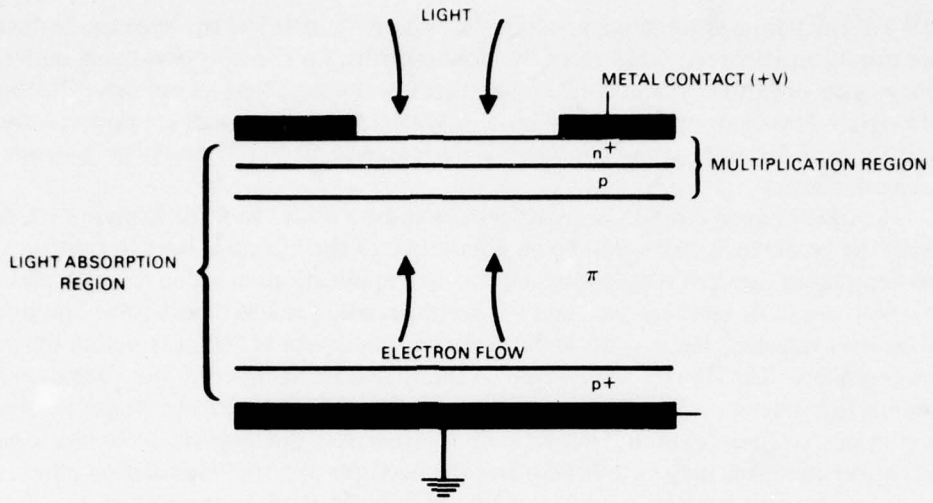

Figure 3. Schematic diagram of a silicon avalanche photodiode. The incident light is absorbed primarily in the wide intrinsic (π) region, creating electron-hole pairs. Carrier multiplication occurs in the high-field depletion region of the pn^+ junction.

so that the avalanche device is characterized by internal gain. Some of the PIN photodiodes will respond at frequencies to several gigahertz, while avalanche devices have cutoff frequencies as high as 1 gigahertz.

Silicon photodiodes are the prevalent type of detector used in multimode fiber communications systems, and the development of digital and analog receivers containing PIN and avalanche devices as well as amplifiers and other electronic elements has been stimulated by the emergence of a fiber-communications industry. Among laboratory devices not yet commercially available, performance at gigahertz frequencies has been obtained in gallium arsenide avalanche photodiodes. Substantial progress has also been made in silicon and gallium arsenide photodiodes coupled to optical waveguides. However, efficient optical coupling is much more easily accomplished with commercial silicon photodiodes, which generally perform better than present guided-wave photodetectors and are therefore preferred in most cases for use with guided-wave devices. Eventually, improved waveguide-coupled diodes could provide performance and cost advantages over conventional detectors in some applications. Finally, although photoemissive detectors are not usually practical for use with guided-wave devices on the basis of size, cost, and high-voltage requirements, they can be useful in the laboratory for device evaluation. Photomultipliers have sensitivity comparable to or better than silicon detectors at visible wavelengths (0.4–0.7 μm), and crossed-field photomultipliers have cutoff frequencies as high as 5 gigahertz, well in excess of most solid-state detectors.

The sensitivity of a receiver, which includes a detector and its following amplifiers, is determined by the efficiency of the detector in converting photons to electrons ("quantum efficiency") and by the various noise factors which can limit the ability of the receiver to restore the original signal.

The detector quantum efficiency q is defined as the average number of photoelectrons generated directly by the absorption of a photon ("primary" photoelectrons) $\bar{n}_e$ to the average number of incident photons $\bar{n}$;

$$q = \frac{\bar{n}_e}{\bar{n}} .$$

For a detector with internal gain G, the average number of collected electrons $\bar{n}_e'$ is

$$\bar{n}_e' = G\bar{n}_e .$$

In terms of the incident optical power P, the photon energy $h\nu$, electronic charge e, and photocurrent I, the quantum efficiency can be written

$$q = \frac{h\nu I}{ePG} .$$

Typical values of quantum efficiency for silicon PIN photodiodes are in the 80%–90% range, and for avalanche photodiodes in the 30%–50% range, at wavelengths near 0.8 μm. At 0.63 μm, the quantum efficiencies are roughly half these figures for solid-state detectors, and 20–30% for photomultipliers. Gains for silicon avalanche photodiodes usually lie in the 50–200 range for optimum performance.

Noise-in-signal is the factor which dictates the best performance which could possibly be obtained in an optical receiver. This type of noise is present because optical sources do not generate photons at uniform time intervals. The average rate of photon emission is fixed by external conditions, such as the electrical power supplied to the source, but individual photons are emitted at random times. Mathematically if the average number of photons per second emitted by the source is N, the probability that n photons will be emitted during any time interval of length τ is given by the following Poisson distribution.

$$P(n,\bar{n}) = \frac{(\bar{n})^n}{n!} e^{-\bar{n}} \qquad (1)$$

where $\bar{n} = N\tau$ is the average number of photons emitted during a time τ.

Light emitted by the source will be attenuated as a result of intervening optical elements and geometrical factors before it reaches a detector, and not all of the photons incident upon the detector will generate photoelectrons. Photons arrive at the detector and generate photoelectrons at random times, so the Poisson distribution describes the electrical output of the photodetector as well as the optical output of the source. For the detection process, $\bar{n}$ is the average number of photoelectrons generated per time interval, and the distribution (1) gives the probability that n photoelectrons will be generated during a time interval.

The "quantum noise limit" of detection of transmitted binary data can be calculated immediately from (1). It is assumed that a train of "ones" and "zeros" is generated by an optical transmitter, that an average of $\bar{n}$ photons is detected by an "ideal" (ie, noise-free) receiver during a time interval if a "one" was transmitted, and that no photons are detected if a "zero" was transmitted. The detector output then passes through a decision circuit, which generates a "one" if one or more photons are detected during a time τ, and a "zero" if no photons are detected. The probability of error P_E is then given by

$$P_E = \frac{1}{2} P(0,\bar{n}) = \frac{1}{2} e^{-\bar{n}} \qquad (2)$$

assuming that "ones" and "zeros" are equally likely to be transmitted. The average number of detected photons per time interval needed to achieve this error rate, $\bar{n}_E$, is then given by

$$\bar{n}_E = -\frac{1}{2} \ell n\,(2P_E) \tag{3}$$

which corresponds to an optical power P incident on the detector of

$$P = \frac{h\nu\bar{n}_E}{\tau} = \frac{h\nu}{2q\tau}|\ell n(2P_E)| \,. \tag{4}$$

This represents the minimum power at a particular optical frequency which is needed to receive data at a rate of $1/\tau$.

In practice, of course, solid-state optical receivers do not perform to the quantum limit given by (4). Dark current shot noise and amplifier noise (including thermal noise) can also limit the receiver performance. However, in avalanche photodiode receivers, the internal gain can, in effect, boost the signal above most of the amplifier noise. Dark current in the best devices can also be quite low. As a result, avalanche photodiode receivers with sensitivity within about 15 dB of the quantum limit have been fabricated for data rates from 1–800 Mb/s. A comparison of the performance of state-of-the-art receivers using silicon PIN and silicon avalanche photodiodes[4] with the quantum limit is given in fig 4, for an assumed error rate of 10^{-9}. It is probable that, in the future, receivers using solid-state detectors will move a few dB closer to the quantum limit, but dramatic improvements should not be expected.

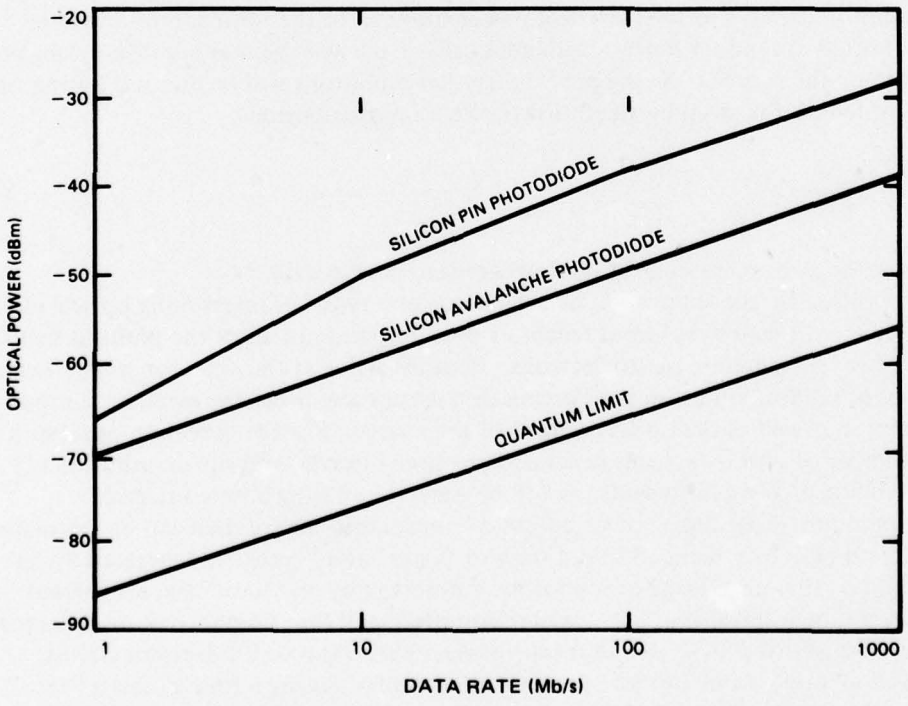

Figure 4. Comparison of state-of-the-art receiver performance with the quantum limit. The internal gain of the silicon avalanche photodiode gives an improvement of about 10 dB in sensitivity in comparison with the silicon PIN photodiode for data rates between 10 Mb/s and 1 Gb/s. The avalanche photodiode sensitivity is nearly 20 dB less than the quantum limit, which assumes a noiseless receiver with unity quantum efficiency.

C. OPTICAL MODULATORS AND SWITCHES

An applied electric or magnetic field or an acoustic wave can affect the propagation of a guided light beam. The amplitude, phase, or frequency of the wave can be modulated, or the propagation path of a portion of the wave can be displaced spatially. Mathematically, the modulation or switching effect is described in terms of a perturbation in the refractive index of the material, induced by an electro-optic, magneto-optic, or acousto-optic interaction. Some types of guided-wave acousto-optic and electro-optic modulators which are needed for the devices described in section III are discussed below.

1. ACOUSTO-OPTIC MODULATORS

The most useful types of acousto-optic guided-wave devices consist of a planar optical waveguide in which light interacts with a surface acoustic wave, as illustrated in fig 5.[12,13] Waveguides for these devices have been produced by depositing a glass film on a quartz substrate and by diffusing a metallic impurity into lithium niobate. The sound wave generated by one or more interdigital transducers deposited on the surface of the substrate or waveguide sets up a spatially periodic perturbation of the refractive index of the material. This phase grating in the material causes a portion of the guided light wave to be deflected. An important property of the grating is its momentum vector, $\bar{k}_g$, which coincides with the direction of acoustic wave propagation and is equal in magnitude to $2\pi/\Lambda$, where Λ is the acoustic wavelength. The propagation vector of a diffracted light wave $\bar{\beta}_d$ is related to that of the incident (zeroth-order) wave $\bar{\beta}_o$ by the equation

$$\bar{\beta}_d = \bar{\beta}_o \pm \ell\, \bar{k}_g \tag{5}$$

where ℓ represents the diffraction order. This expression can be decomposed into two equations

$$(\beta_d)_\perp = (\beta_o)_\perp \tag{6}$$

$$(\beta_d)_\parallel = (\beta_o)_\parallel \pm \ell\, k_g, \tag{7}$$

where the subscripts $\perp$ and $\parallel$ refer to the component of $\bar{\beta}$ perpendicular to and parallel to the direction of acoustic propagation, respectively. These equations are satisfied only if

$$\theta_d = 2 \tan^{-1}\left(\frac{\ell\, k_g}{2\beta_o}\right) \tag{8}$$

where θ_d is the angle between $\bar{\beta}_o$ and $\bar{\beta}_d$, and if the vector $\bar{\beta}_o + \bar{\beta}_d$ is perpendicular to $\bar{k}_g$, as indicated in fig 6. If these conditions are satisfied, the effect is known as Bragg diffraction. Usually the first-order diffraction ($\ell = 1$) is much stronger than higher orders ($\ell = 2,3,\ldots$). If this is true, and if the light wave propagates in a direction nearly normal to the direction of acoustic propagation, then (8) reduces to

$$\theta_d \approx \frac{\lambda}{n\Lambda} \tag{9}$$

---

[12]Kuhn, L, Dakss, ML, Heidrich, PF, and Scott, BA, "Deflection of an Optical Guided Wave by a Surface Acoustic Wave," Appl Phys Lett, v 17, p 265-267, September 15, 1970

[13]Tsai, CS, Alhaider, MA, Nguyen, LT, and Kim, B, "Wide-band Guided-Wave Acousto-optic Bragg Diffraction and Devices Using Multiple Tilted Surface Acoustic Waves," Proc IEEE, v 64, p 318-327, March 1976

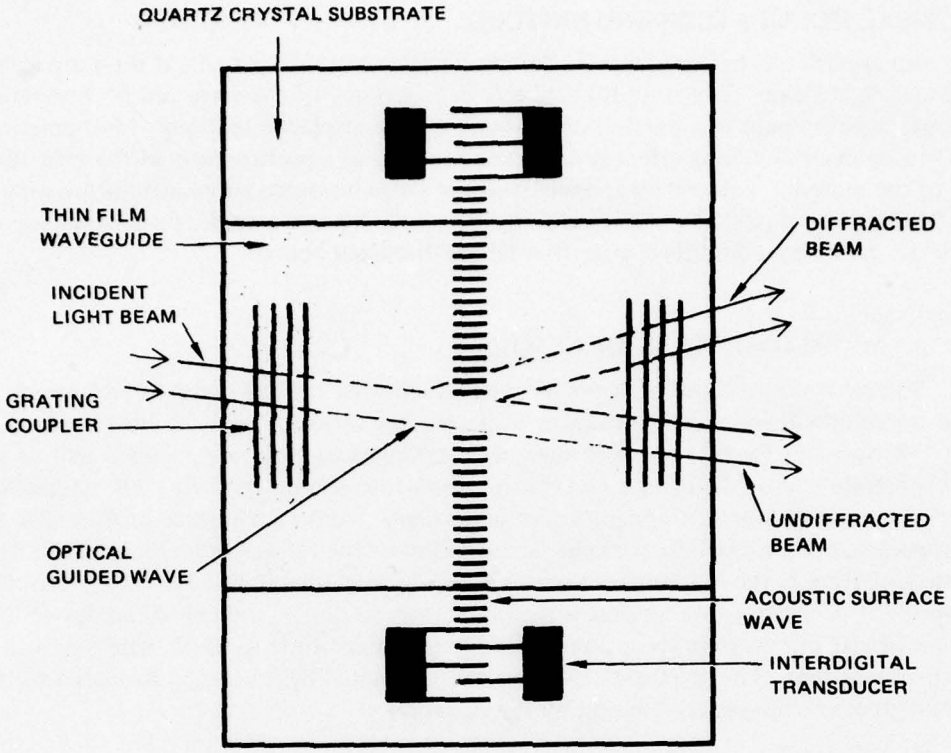

Figure 5. Schematic diagram of an acousto-optic surface wave beam deflector.

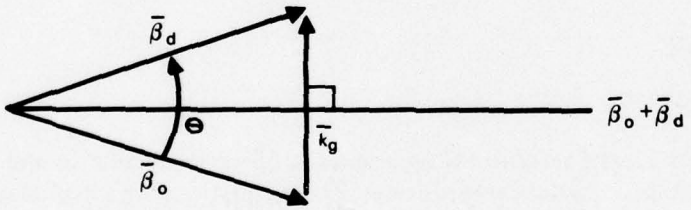

Figure 6. Wave-vector diagram for a Bragg acousto-optic modulator.

where λ is the free-space wavelength and Λ is the refractive index of the waveguide. This relation refers to the angle between incident and diffracted waves in the waveguide. In air, the angle is larger by a factor equal to the refractive index of the material, so that

$$(\theta_d)_{air} \approx \frac{\lambda}{\Lambda}. \tag{10}$$

A useful feature of the acousto-optic modulator is that the deflection angle θ_d can be changed by varying the acoustic frequency. The acoustic wavelength is given by

$$\Lambda = \frac{V}{\nu} \tag{11}$$

where ν is the acoustic frequency and V is the sound velocity ($V \sim 3 \times 10^5$ cm/s in most materials). For a central acoustic frequency of 500 MHz, a material refractive index of 2.2 (corresponding to lithium niobate), and an optical wavelength of 0.63 μm (corresponding to the helium neon laser), the deflection angle in air calculated from (10) is $\theta_d = 0.095$ radian (5.3°), and varying the frequency by ± 100 MHz causes θ_d to vary from 6.8° to 4.3°.

By passing the light from an acousto-optic modulator through a lens, the undiffracted and diffracted beams can be focused to small spots. The location of one of these spots in the focal plane of the lens is determined by the angle at which the corresponding wave emerges from the device. As the acoustic frequency varies, the position of the focused spot corresponding to the diffracted wave will change, and if more than one frequency is present in the acoustic wave, spots corresponding to each of these frequencies will be present simultaneously. The number of resolvable spots (or frequencies) N is given approximately by the effective width W of the acousto-optic interaction region, expressed in acoustic wavelengths; that is,

$$N \approx W/\Lambda.$$

The primary factors which can limit W are the width of the optical beam and the acousto-optic attenuation factor.

2. ELECTRO-OPTIC MODULATORS

A feature of electro-optic waveguide modulators and switches which makes them attractive for many devices is that they can be fabricated in a "channel waveguide" configuration. The channel waveguide confines a beam in both transverse dimensions, rather than in one dimension as in the case of a planar waveguide. This is important for two reasons: first, the channel waveguide is the only guided-wave structure which is easily interfaced with a single-mode optical fiber; second, the transverse beam confinement makes it possible to minimize the electrical voltage and drive power needed to operate a particular device. Channel waveguide modulators have been fabricated in semiconducting materials such as gallium arsenide and zinc selenide, but the most efficient modulators and switches have been produced by metal diffusion in the ferroelectric insulators lithium niobate and lithium tantalate. These materials have a large electro-optic coefficient and low resistivity and are readily available in large-area crystals. Three types of electro-optic devices which have been demonstrated in a channel waveguide configuration – the relative phase modulator, the interferometric modulator, and the directional coupler switch–are discussed below.

In the relative phase electro-optic modulator, illustrated schematically in fig 7, an applied electric field changes the phase of guided modes of one polarization relative to the guided modes of an orthogonal polarization.[14,15] This phase modulation can be converted to intensity modulation by passing the light beam emerging from the modulator through an analyzer, which transmits only one linearly polarized component. The intensity of the light transmitted by the analyzer, I, is given by

$$I = A + B \cos^2 (\Delta\Gamma + \Gamma_o), \tag{12}$$

---

[14]Kaminow, IP, "Optical Waveguide Modulators," IEEE Trans Microwave Theory and Tech, v MTT-23, p 57-70, January 1975

[15]Kaminow, IP, and Turner, EH, "Electro-optic Light Modulators," Proc IEEE, v 54, p 1374-1390, October 1966

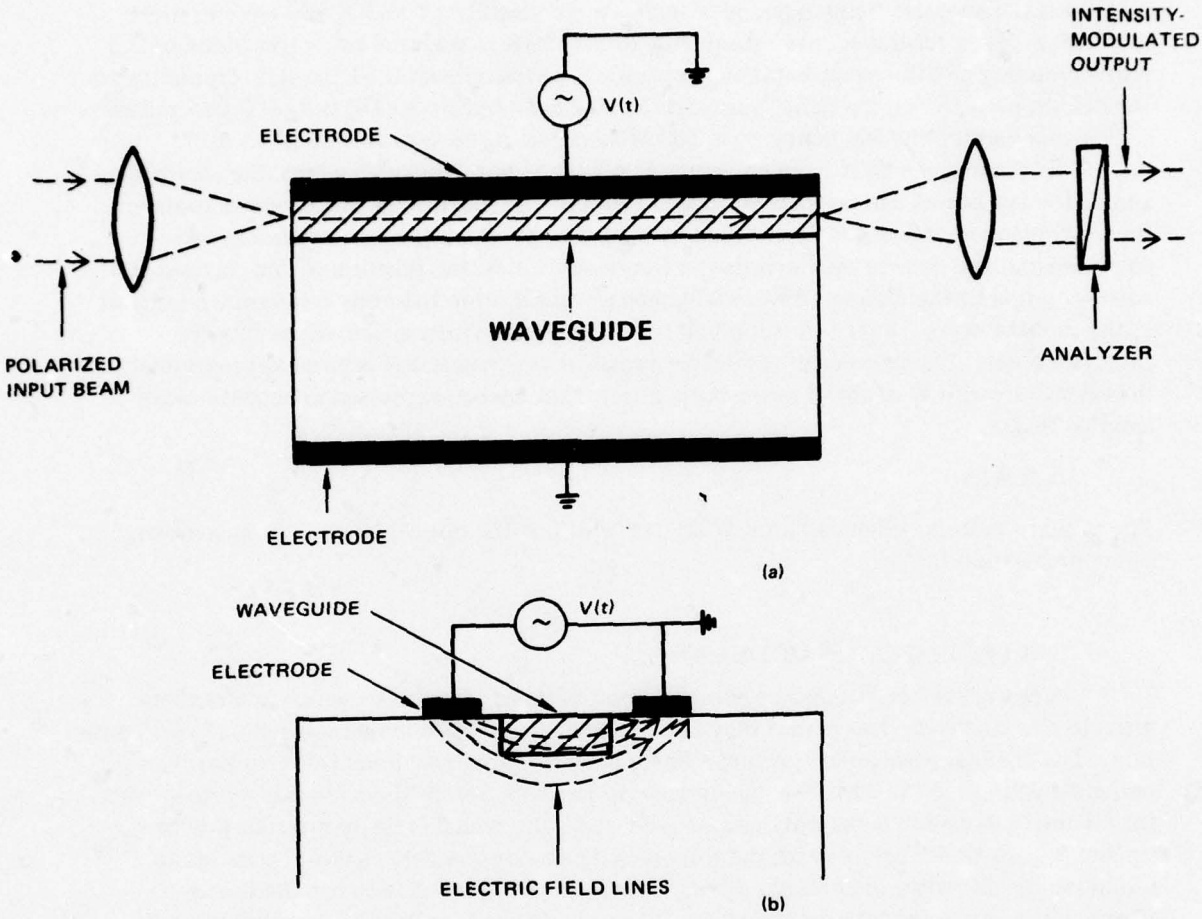

Figure 7. Relative phase electro-optic modulator: (a) planar waveguide, (b) channel waveguide. In both cases, the analyzer converts the phase-modulated output of the waveguide to intensity modulation.

where $\Delta\Gamma$ is the induced electro-optic phase shift, Γ_o is a phase shift which occurs in the absence of an applied field, and A and B are constants which depend on the total light output of the modulator, the polarization of the beam incident on the modulator, and the orientation of the analyzer. Maximum depth of modulation is usually obtained if the polarization of the incident beam is oriented at 45° to the axes of the crystal and the analyzer is oriented to pass light polarized at an angle of 45° to those axes. The orientation of the polarization vector of the input beam and of the analyzer can be adjusted independently to maximize the depth of modulation, such that $B/A >> 1$ and the modulation depth approaches 100%.

The materials of interest for guided-wave devices, such as lithium niobate and gallium arsenide, demonstrate the Pockels effect, in which the refractive index change is a linear function of the applied electric field. In this case, $\Delta\Gamma \sim V$, where V is the applied voltage. The depth of modulation can often be improved by applying a dc bias voltage V_d as a means of canceling the static phase shift, that is, so that $\Delta\Gamma_d + \Gamma_o = N\pi$, where N is an integer. The modulating voltage V is then superimposed on the dc bias.

In the interferometric modulator, a branching waveguide beam splitter causes a separation of the incident light wave into two spatially distinct paths.[16,17] An applied electric field induces a relative phase change $\Delta\Gamma$ between those two beams, which are then recombined by a second beam splitter, as illustrated in fig 8. The two beams can interfere constructively or destructively, depending on the value of the relative phase difference. The resultant optical output of the second beam splitter is once again described by (12), where the constants A and B depend on the total incident light intensity and the optical transmission of the device, and upon the beam splitter characteristics. Best performance is obtained for beam splitters which divide the intensity of a beam equally between the two paths; in this case, $B/A >> 1$ and the modulation depth approaches 100%.

The electro-optically induced phase change will in general be different for waves polarized along the two crystal axes. This means that $\Delta\Gamma_1 = K_1V$ and $\Delta\Gamma_2 = K_2V$, where V is the applied voltage and K_1 and K_2 are constants determined by material and device characteristics. Since intensities of the two polarization components are modulated independently, complete extinction will not generally be obtained unless the incident beam is polarized along one of the waveguide axes. Best performance is obtained for a polarization along the axis with the largest electro-optic effect.

An important advantage of the interferometric modulator is that no analyzer is needed. A further advantage is that it is relatively temperature insensitive. Variations in the

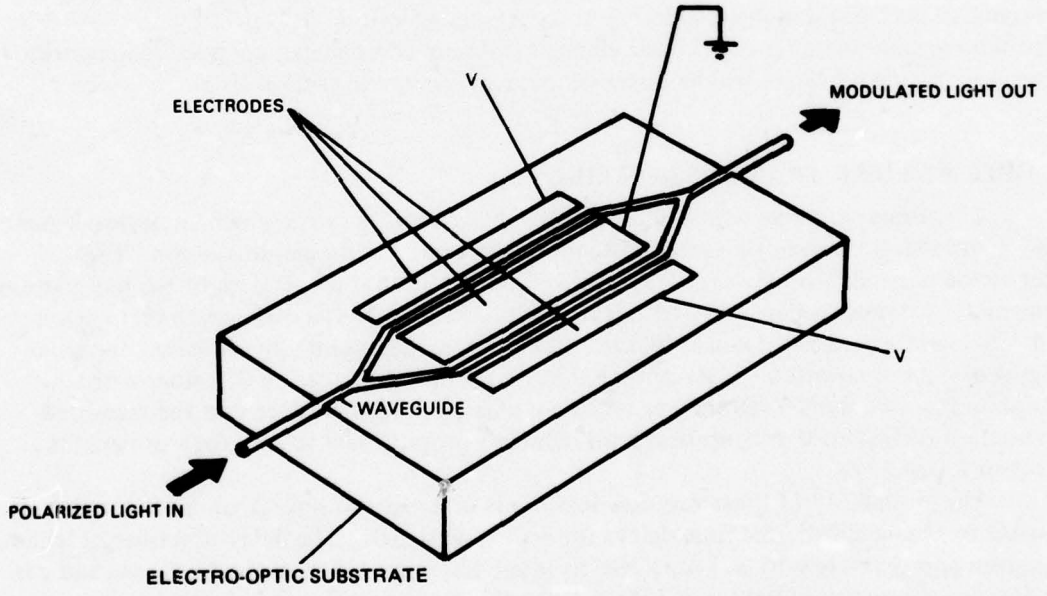

Figure 8. Interferometric electro-optic modulator. The applied electric field changes the phase of the light wave in one branch of the interferometer relative to the other branch. Recombination of these branches converts the phase modulation to intensity modulation.

---

[16]Martin, WE, "A New Waveguide Switch/Modulator for Integrated Optics," Appl Phys Lett, v 26, p 562-564, May 1975

[17]Ohmachi, Y, and Noda, J, "Electro-optic Light Modulator With Balanced Bridge Waveguide," Appl Phys Lett, v 27, p 544-546, November 1975

ambient temperature can cause wide fluctuations in the static phase shift in the relative phase modulator, but, in the interferometric modulator, these changes will cancel because the two spatially separated beams are affected equally.

In the coupled waveguide electro-optic switch[18–20] illustrated in fig 9, the applied field affects the coupling of optical power between two parallel waveguides. The waveguides are physically very close to one another (ie, within a few wavelengths) throughout the length of a coupling region, and are made as nearly identical as possible. In the absence of an applied field, the propagation constants for the guided modes in the two waveguides are approximately the same, and optical power injected into one waveguide will couple efficiently to the second guide. Complete power transfer will occur in a distance L, called the coupling length. In this case, the waveguides are said to be synchronous. When a field is applied, the waveguides are no longer synchronous (ie, the guided-mode propagation constants are no longer identical). This causes the power transfer to be less efficient, and the coupling length to become shorter. For a particular value of the applied voltage, V_0, it is possible to switch all of the power back to the initially excited waveguide. If the effective length of the waveguide coupling region is equal to L, the coupling length in the absence of the applied field, then complete switching of the output from one waveguide to another can occur.

For one state of the switch, with no applied voltage, light injected into one waveguide will emerge from the second waveguide. In the other state of the switch, with the voltage equal to V_0, light injected into a particular waveguide will emerge from the same waveguide. Thus, the operation of the synchronous waveguide optical switch is analogous to the familiar electrical double-pole double-throw reversing switch. It is possible to use 2 X 2 optical waveguide switches as the basic elements in more complicated connecting networks. Optical switching networks will be discussed in greater detail in section III-E.

D. OPTICAL FIBER TRANSMISSION LINE

The primary factors which determine the length of fiber over which an optical signal can be successfully transmitted are its attenuation per unit length and dispersion. The attenuation depends strongly on the optical wavelength but is independent of the modulation frequency. Attenuation in silica and silicate fibers of 1 dB/km at a wavelength of 1.06 μm (Nd:YAG laser wavelength) and 2 dB/km at 0.8 μm (gallium aluminum arsenide laser wavelength) have been reported.[21] Recent data on the spectral attenuation of a fiber with a minimum loss of only 0.5 dB/km (see ref 6) are plotted in fig 10. Note that the measured attenuation is close to the theoretical limit, which is proportional to λ^{-4}, for wavelengths less than 1.1 μm.

The availability of these very-low-loss fibers in lengths of several kilometres makes it possible to obtain substantial time delays for wideband signals. The delay of a fiber of length L is given approximately by $n_1 L/c$, where n_1 is the refractive index of the fiber core and c is the free-space velocity of light ($c = 3.00 \times 10^8$ m/s). In fused silica ($n = 1.46$), the delay is

---

[18]Campbell, JC, Blum, FA, Shaw, DW, and Lawley, KL, Appl Phys Lett, v 27, p 202-205, August 15, 1975

[19]Papuchon, M, Combewale, V, Mathieu, X, Ostrowsky, DB, Reiber, L, Roy, AM, Sejourne, B, and Werner, M, "Electrically Switched Optical Directional Coupler – Cobra," Appl Phys Lett, v 27, p 289-91, September 1, 1975

[20]Kogelnik, A and Schmidt, RV, "Switched Directional Couplers with Alternating $\Delta\beta$," IEEE J Quant Electron, v QE-12, p 396-401, July 1976

[21]Tasker, GW, and French, WG, "Low-loss Optical Waveguides With Pure Fused SiO_2 Cores," Proc IEEE, v 62, p 1281-1282, September 1974

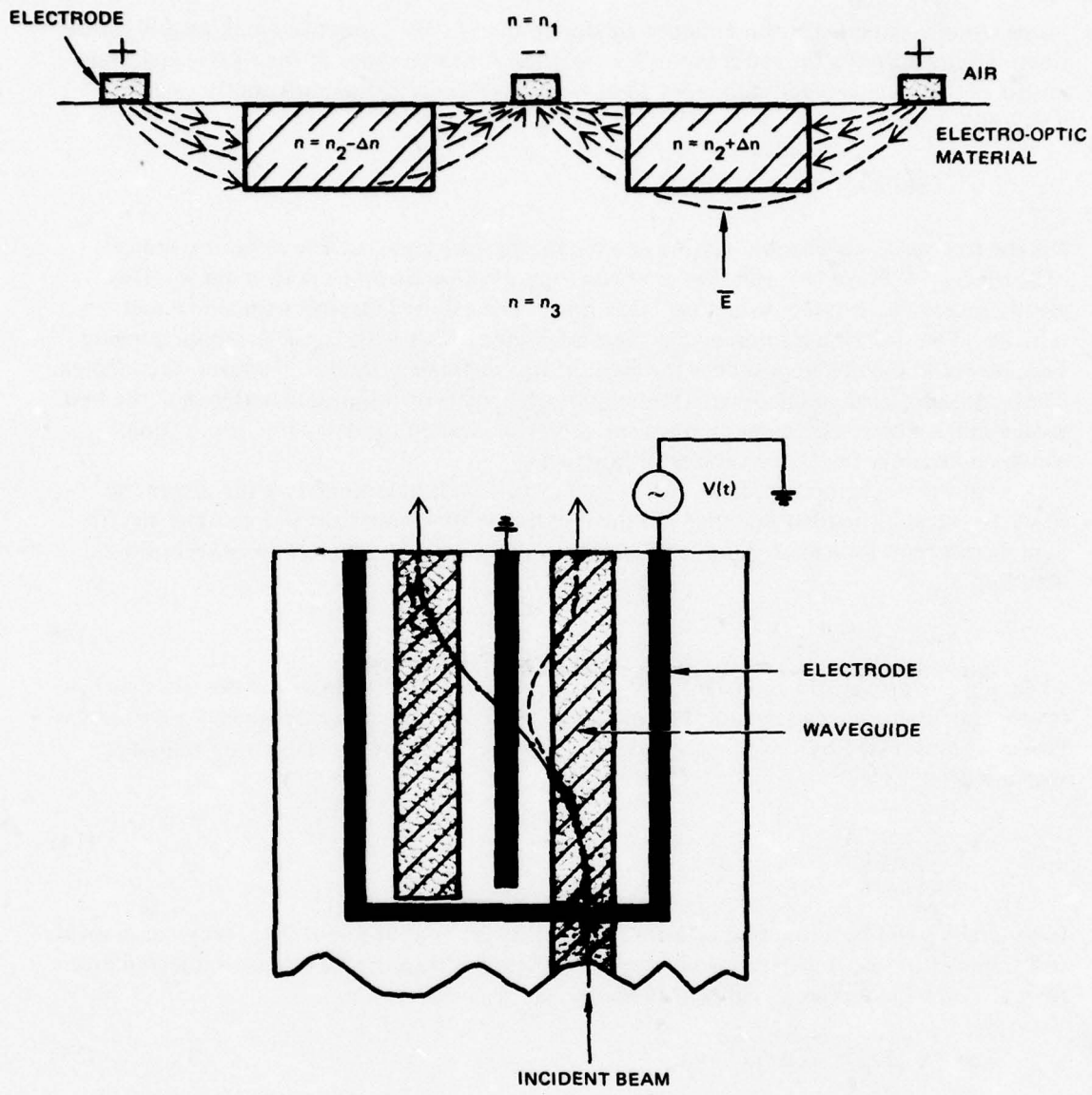

Figure 9. Electro-optic directional coupler 2 × 2 switch. In the absence of an applied field, the waveguides are synchronous, and light injected into one couples into the adjacent one. An applied field spoils the synchronism and the light tends to remain in the initially excited waveguide.

4.9 μs/km. As an example, a maximum delay of 196 μs could be achieved in a fiber with an attenuation of 1 dB/km and an allowable attenuation of 40 dB.

Propagation through a long fiber causes an injected signal to be distorted as well as attenuated. Signal distortion in an optical fiber depends on the number of guided modes and their dispersion characteristics, on the dispersion of the fiber material, and on the spectral width of the light source. The number of guided modes and the field distributions and

propagation constants for those modes are determined by the refractive index profile for the fiber. Figure 11 plots the refractive index variation for three types of fiber for signal transmission.[5] The single-mode step-index fiber must have a core radius sufficiently small at $u \leq 2.405$, where

$$u = 2\pi(a/\lambda)\sqrt{n_1^2 - n_2^2},$$

λ is the free-space wavelength, and n_1 and n_2 are the core and cladding refractive indices, respectively.[22] For $u > 2.405$, the fiber can support more than one guided mode. This greatly increases the pulse distortion, since power in each mode travels with a different velocity. The situation is improved in the graded index fiber with a near-parabolic profile, since power in the different modes travels at nearly the same velocity. However, the inherent bandwidth of a single-mode fiber is still one to two orders of magnitude better than the best graded-index fibers. Single-mode fibers are therefore needed for delay-line applications which require very high time-bandwidth products.

In the single-mode optical fiber, signal distortion is determined by the dispersion characteristics of the fiber material and the spectral width of the light source. The electric field distribution for a guided mode of an optical fiber, with its propagation axis in the z-direction, is

$$\bar{E} = \bar{\epsilon}(x,y)e^{i(\omega t - \beta z)} \tag{13}$$

where β is the propagation constant, $\bar{\epsilon}(x,y)$ is the spatial distribution of the electric field vector for the mode, and the radian frequency ω is related to the optical frequency ν by $\omega = 2\pi\nu$. Power is transmitted by the guided mode at a velocity V_g, known as the group velocity, which is given by

$$V_g = \frac{1}{\left(\frac{\partial\beta}{\partial\omega}\right)}. \tag{14}$$

In general V_g will be a function of optical frequency, so that different frequency components will transmit power at different velocities. If a pulse with spectral width $\Delta\nu$ is injected into a fiber at $z = 0$, the temporal width of the pulse, $\Delta\tau$, is given by

$$\Delta\tau = \sqrt{(\Delta\tau_o)^2 + (\Delta\tau_1)^2} \tag{15}$$

where $\Delta\tau_o$ is the width of the incident pulse and $\Delta\tau_1$, the pulse broadening due to dispersion in the fiber, is

$$\Delta\tau_1 = \left| Z\frac{\partial}{\partial\nu}\left(\frac{1}{V_g}\right)\Delta\nu \right| = \left| \frac{z}{V_g^2}\frac{\partial V_g}{\partial\nu}\Delta\nu \right|. \tag{16}$$

Two factors, dispersion of the fiber material and dispersion attributable to the waveguide structure, determine the value of $\partial V_g/\partial\nu$, but material dispersion is the dominant factor in

---

[22]Snitzer, E, "Cylindrical Dielectric Waveguide Modes," J Opt Soc Amer, v 51, p 491-498, May 1961

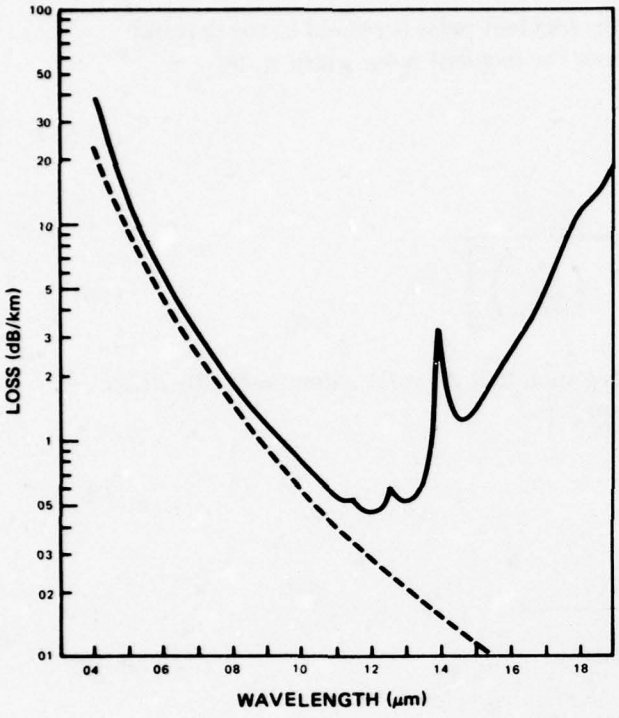

Figure 10. Spectral loss characteristics for a low-loss fiber with a phosphosilicate core and a borosilicate cladding. The dashed line represents a theoretical minimum loss resulting from Rayleigh scattering for this type of fiber.

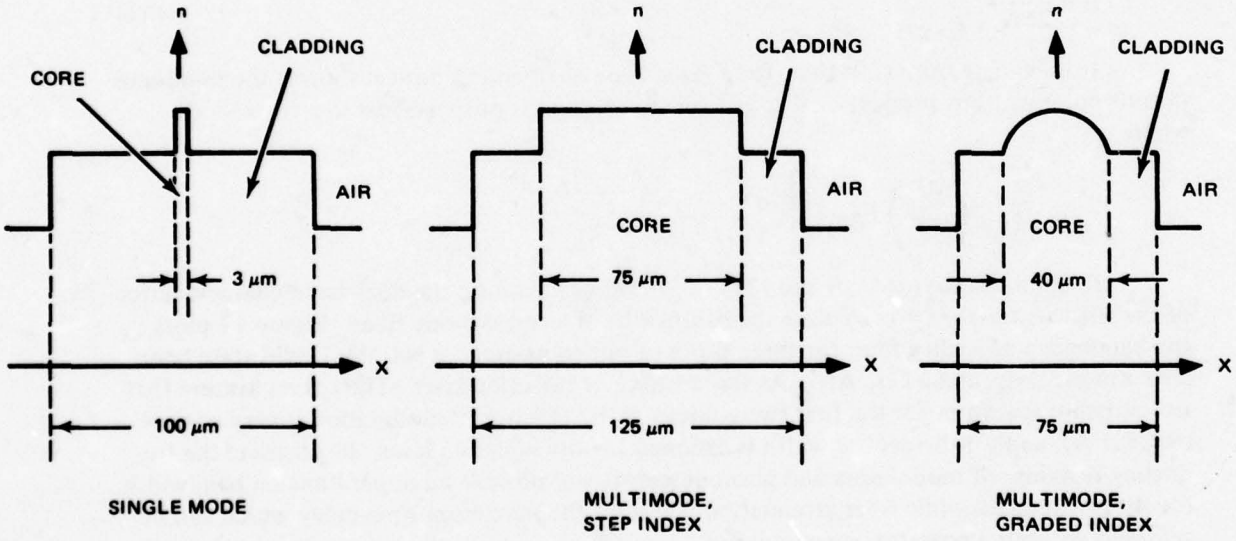

Figure 11. Refractive index profiles for three types of optical fibers for signal transmission. Typical core and cladding dimensions are indicated.

single-mode fibers. The spectral width $\Delta\nu$ of the incident pulse is related to the spectral width $\Delta\nu_s$ of the unmodulated optical source and the incident pulse width τ_o by

$$\Delta\nu = \sqrt{(\Delta\nu)_s^2 + \left(\frac{1}{2\pi\tau_o}\right)^2} \tag{17}$$

so that the expression for $\Delta\tau$ becomes

$$\Delta\tau = \sqrt{(\Delta\tau_o)^2 + \frac{z^2}{V_g^4}\left(\frac{\partial V_g}{\partial\nu}\right)^2 \left[(\Delta\nu_s)^2 + \left(\frac{1}{2\pi\tau_o}\right)^2\right]}. \tag{18}$$

For a given value of z, there exists a value of $\Delta\tau_o$ such that $\Delta\tau$ (z) is a minimum. By differentiating (18), it can be shown that, for minimum $\Delta\tau$

$$\Delta\tau_o = \sqrt{\left(\frac{1}{2\pi}\right)\frac{z}{V_g^2}\frac{\partial V_g}{\partial\nu}} \tag{19}$$

and the corresponding pulse width is

$$\Delta\tau = \sqrt{\frac{1}{\pi}\left(\frac{z}{V_g^2}\right)\frac{\partial V_g}{\partial\nu} + \frac{z^2}{V_g^4}\left(\frac{\partial V_g}{\partial\nu}\right)^2 (\Delta\nu_s)^2}. \tag{20}$$

The bandwidth B of a section of fiber of length z can be expressed in terms of $\Delta\tau$ as

$$B = \frac{1}{2\pi\Delta\tau}. \tag{21}$$

It is evident from (20) that, for a given type of fiber and optical source, the minimum output pulse width is proportional to $\sqrt{z}$ for $z \ll z_o$ and is proportional to z for $z \gg z_o$, where

$$z_o = V_g^2\left[\pi\left(\frac{\partial V_g}{\partial\nu}\right)(\Delta\nu_s)^2\right]^{-1}.$$

It is possible to use (20) and (21), together with data on the dispersion characteristics of the fiber material,[23] to calculate the bandwidth of a single-mode fiber. Figure 12 plots the bandwidth of a silica fiber for three types of optical source: a Nd:YAG solid state laser, a Kr:ion gas laser, and a $Ga_x\ Al_{1-x}As$ semiconductor injection laser. The curves assume that the emission spectrum for the first two sources in the absence of modulation is very narrow ($\ll$ 0.1 Å), and a 1-Å spectral width is assumed for the injection laser. In practice, the frequency response of modulators and photodetectors will provide an upper limit on bandwidth for short distances, while fiber attenuation will limit the maximum time delay which can be achieved without a repeater or recirculator.

[23] Jurgensen, K, "Dispersion-Optimized Optical Single Mode Glass Fiber Waveguides," Appl Opt, v 14, p 163-168, Jan 1975

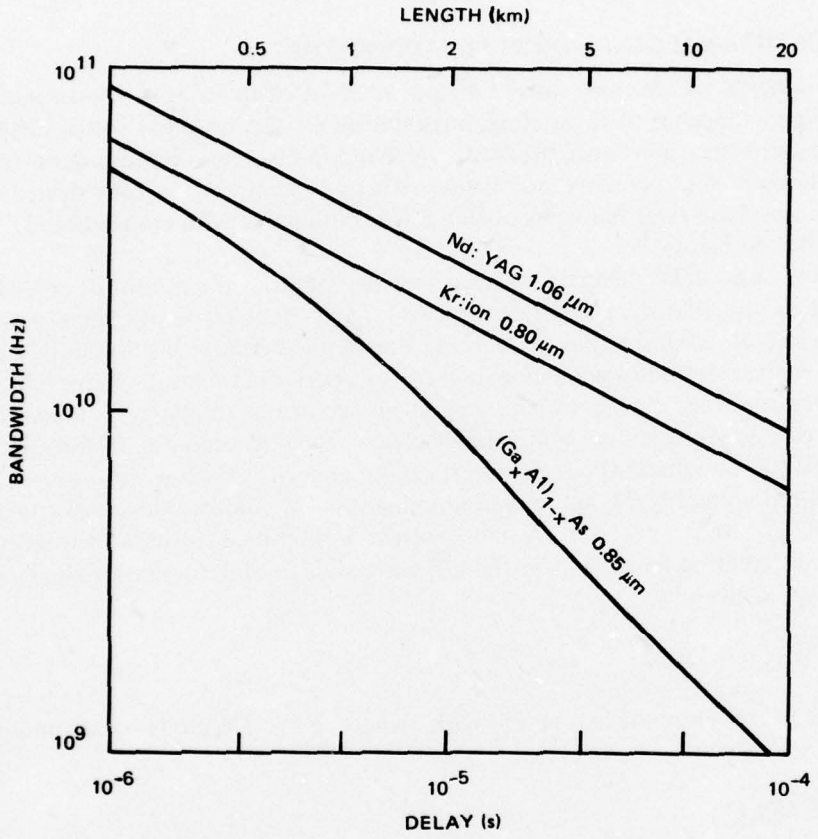

Figure 12. Bandwidth of a single-mode optical fiber made of fused silica plotted as a function of time delay and fiber length, for three types of optical source. The Nd:YAG and Kr:ion lasers are assumed to emit a monochromatic (single frequency) line, while the spectral width of the $Ga_x\ Al_{1-x}As$ laser is assumed to be 1 Å.

III. SIGNAL PROCESSING DEVICES AND SUBSYSTEMS

This section describes optical devices for performing the signal processing functions of analog-to-digital conversion, signal delay, pseudorandom sequence generation, rf spectrum analysis, and switching. In each use, a comparison is made with present or alternative methods of performing the same function. Applications for these devices are discussed in section IV.

A. ELECTRO-OPTIC ANALOG-TO-DIGITAL CONVERTER

Analog-to-digital (A/D) converters[24,25] are widely used to translate sensor measurements into the digital language of computing, information processing, and control systems. Some of these systems (eg, signal processors for wideband radars) are limited in performance by the speed of present electronic A/D converters. A new type of electro-optic device which offers potential conversion rates in excess of those now obtainable with conventional techniques is described below.[26]

The electro-optic A/D converter makes use of the fact that the output of an optical intensity modulator, the operation of which is based on a linear electro-optic phase retardation,[14,15] varies in periodic fashion as a function of an applied voltage V. Similarly, each bit in the binary representation of an analog quantity is a periodic function of the value of that quantity. The proposed device, which takes advantage of this similarity, is illustrated schematically in fig 13. An array of identical dielectric channel waveguides is fabricated in a single-crystal substrate of a linear (Pockels) electro-optic material. Each waveguide, which can support one predominantly TE and one predominantly TM guided mode, is excited by linearly polarized light from a cw laser. A signal voltage V is applied across each waveguide. The electro-optic interaction length L_n for the n^{th} waveguide, as determined by the length of the signal electrode, is given by

$$L_n = 2^{n-1} L_1, \; n = 1,2,3,\ldots$$

The phase of light in the TE mode is retarded with respect to the TM mode by an amount $\Delta\Gamma_n$ given by

$$\Delta\Gamma_n = 2^{n-1} K L_1 V.$$

The value of the constant K is determined by the electro-optic coefficients of the material, the waveguide parameters, and the electrode spacing. The light from each waveguide is passed through a polarization separator, (eg, a Rochon or Wollaston prism), and the intensities of two orthogonally polarized components are detected separately. These intensities are given by

$$I_{na} = A_n \cos^2 (\Delta\Gamma_n/2 + \psi_n) + B_n \qquad (22)$$

---

[24]Hoeschele, DF, Jr, Analog-to-Digital/Digital-to-Analog Conversion Techniques, New York, Wiley, 1968

[25]Sheingold, DH, and Ferrero, RA, "Understanding A/D and D/A Converters," IEEE Spectrum, v 9, no 9, p 47-56, September 1972

[26]Taylor, HF, "An Electro-optic Analog-to-Digital Converter," Proc IEEE v 63, p 1524-1525, October 1975

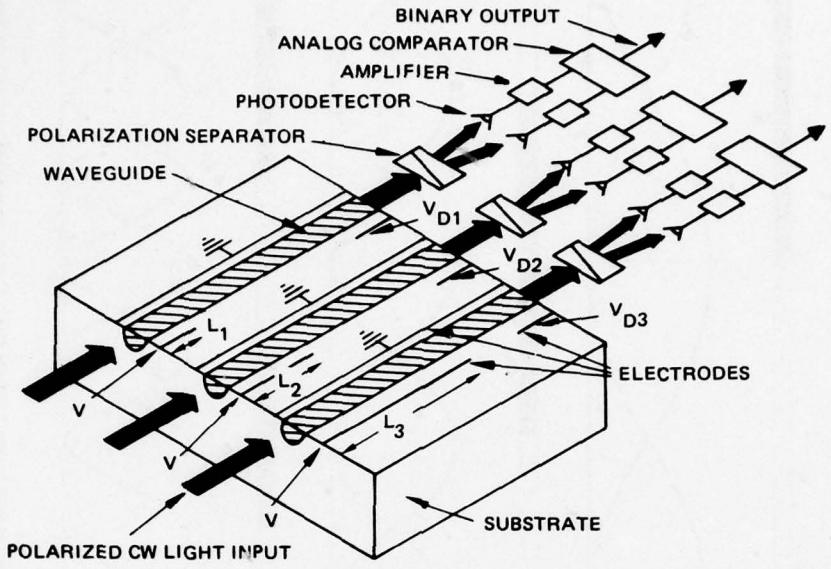

Figure 13. Schematic diagram of a three-bit electro-optic A/D converter.

$$I_{nb} = A_n \sin^2 (\Delta\Gamma_n/2 + \psi_n) + C_n, \tag{23}$$

where ψ_n is a static phase shift, A_n is the modulation amplitude, and B_n and C_n are dc terms which can be removed from the detector signals by filtering or subtraction. The modulation amplitude can be maximized by independently adjusting the orientation of the polarization separator and of the polarization vector of the incident beam.

A binary representation of V is obtained by electronically comparing the intensities I_{na} and I_{nb}, and generating a "one" or "zero" for the n^{th} bit based on the outcome of the comparison. For example, an offset binary code for a bipolar signal[25] is obtained if $\psi_n = \pi/4$ for each n by generating a "one" for the first bit if $I_{1b} > I_{1a}$, and a "one" for the n^{th} bit, n = 2,3, . . . if $I_{na} > I_{nb}$. The required values for all ψ_n are obtained by applying a dc voltage V_{Dn} to a short section of each waveguide. The intensities I_{na} and I_{nb} and the corresponding offset binary code are plotted as a function of V in fig 14 for a device with 3-bit precision. It is evident from fig 14 that, as V changes, it is possible for two or even all three bits to change in value simultaneously. Significant errors in the conversion are most likely to occur for values of V near these intensity crossover points. One way to avoid this problem is to use a Gray scale instead of a pure binary code. The only change from the offset binary device is in values for the static phase shifts (ψ_n). Variations in the intensity components I_{na} and I_{nb} for a 4-bit Gray-scale converter are illustrated in fig 15. Since the value of only one bit

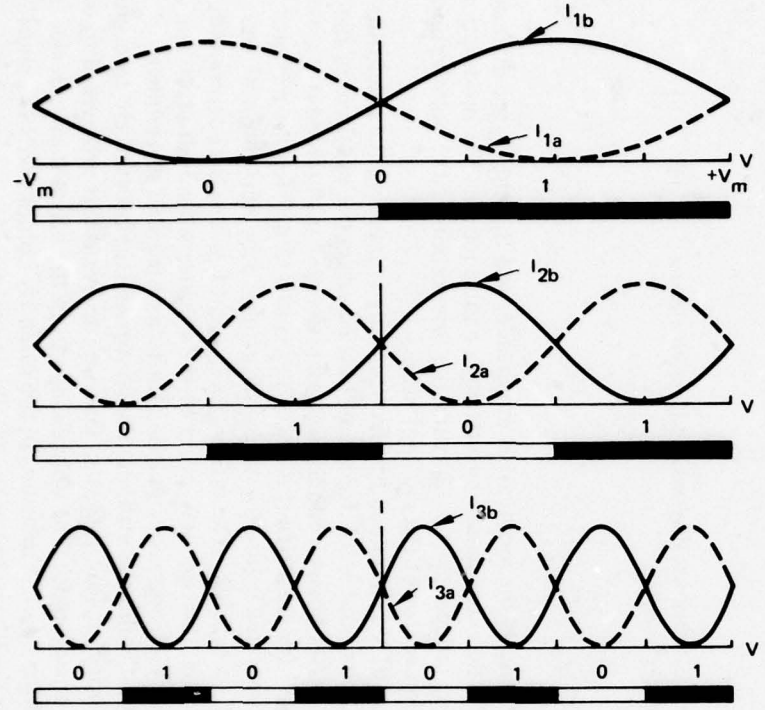

Figure 14. Variation of the intensities of two orthogonally polarized components of light emerging from the waveguide modulators as a function of the applied voltage, V, which can vary from $\pm V_m$. The offset binary representation of V is obtained by comparing I_{na} with I_{nb}.

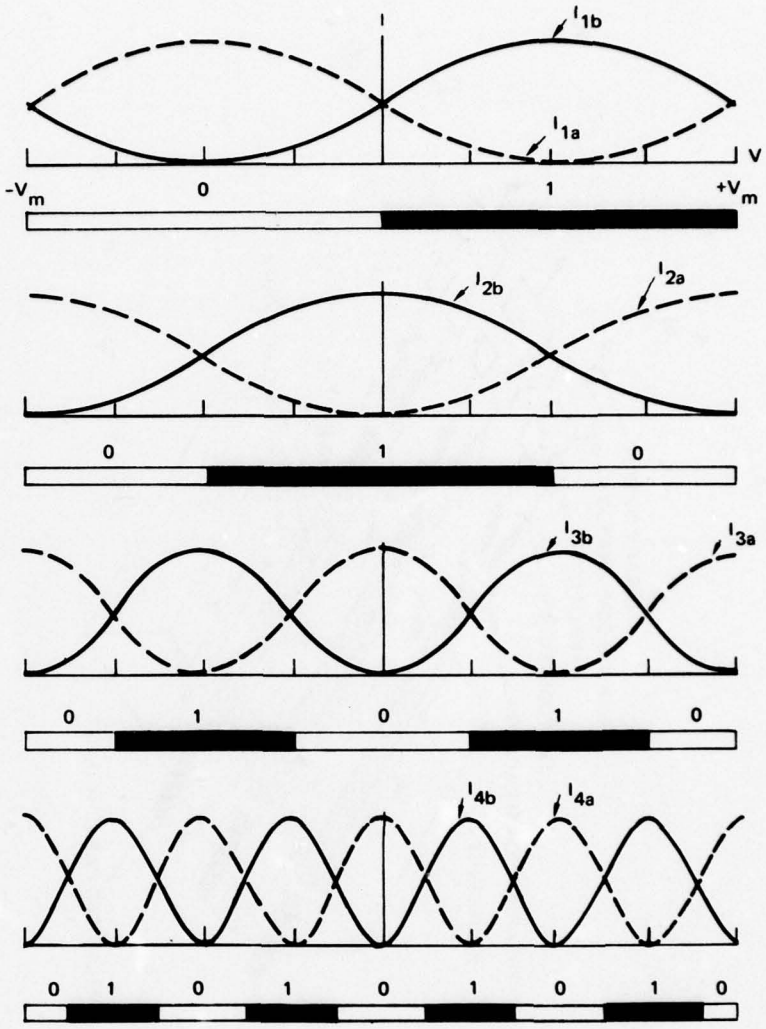

Figure 15. Intensity versus voltage plot for a 4-bit A/D converter with Gray-scale output.

changes for small variations in V, the probability of error in one of the most significant bits is greatly reduced. Furthermore, in a device of given length, one more bit of precision can be obtained with the Gray code than with the offset binary code.

The number of bits of precision, N, which can be obtained with a Gray code is related to the length ℓ of the waveguides according to

$$N = \log_2 (\ell/\ell_\pi) + 2, \tag{24}$$

where ℓ_π is the minimum length required for a pi-radian electro-optic phase retardation. The formula

$$\ell_\pi = V_\pi d/V_m \tag{25}$$

relates ℓ_π to the electrode spacing d, the half-wave voltage V_π of the material, and the maximum applied voltage V_m. (It is assumed that V varies between $\pm V_m$.) As a numerical example, the electro-optic material is assumed to be $LiNbO_3$, oriented with the c-axis in the device plane and perpendicular to the waveguide axes (see fig 13). The value of V_π in that material is 2700 V at 6328 Å for an applied field parallel to the c-axis and propagation perpendicular to that axis.[27] If V_m = 12.5 volts and d = 5μm, corresponding to an average field strength of 25 000 V/cm between the electrodes, the value for ℓ_π is estimated from (25) to be 1.08 mm. According to (24), the length of a 6-bit A/D converter with these parameters is 1.7 cm.

The electrical power required to drive the modulator is an important parameter of the device. This can be calculated from the formula

$$P = \frac{1}{2} C V_m^2 B \tag{26}$$

where B is the modulation bandwidth and C is the electrode capacitance. If the widths of the electrodes and the spacing between them are of equal magnitude, the capacitance is approximately given by

$$C = (\epsilon_o + \epsilon) L \tag{27}$$

where L is the total electrode length, in this case given by

$$L = \sum_{n=1}^{N} Ln. \tag{28}$$

But $L_n = 2^{n-N} \ell$, where ℓ is the length of the longest electrode (equal to the length of the device), so evaluating the sum in 28 yields

$$L \sim 2\ell.$$

But $\epsilon_o = 8.9 \times 10^{-14}$ F/cm and, in lithium niobate, $\epsilon \sim 30\epsilon_o$, so if ℓ = 1.7 cm, then from (27)

$$C = 9.4 \text{ pF}.$$

---

[27]Denton, RT, Chen, FS, and Ballman, AA, "Lithium Tantalate Light Modulators," J Appl Phys, v 38, p 1611-1617, March 15, 1967

For a signal bandwidth of 500 MHz (corresponding to a Nyquist sampling rate of 1 GHz), the power calculated from (26), assuming $V_m \approx 12.5$ V, is $P \sim 360$ mW.

A difficulty encountered in materials with large electro-optic coefficients, such as $LiNbO_3$, is that the static birefringence is strongly dependent on temperature.[27] In the device illustrated in fig 13, it would be necessary to adjust the dc bias voltages V_{Dn} to compensate for ambient temperature variations and for heating of the waveguide material by the rf modulating field. As an alternative, each channel of the A/D converter could employ the modulator structure illustrated in fig 16.[28] The polarization of the incident cw laser beam is oriented for maximum coupling into a particular mode (TE or TM) of one of a pair of parallel waveguides. After the light is split into equal-amplitude components by a 3-dB directional coupler, a phase shift equal in magnitude but opposite in sign is induced in the waveguides by a voltage V applied to the signal electrodes. The two spatial components are then mixed by a second 3-dB coupler, and the output from each waveguide is detected separately. The dependence of the intensities of the two spatial components on the phase retardation $\Delta\Gamma_n$ is once again given by (13) and (14), where, in this case, $\Delta\Gamma_n$ equals the difference in electro-optic phase shifts for the individual waveguides. Variations in temperature will affect the phase of a propagating wave by the same amount in each waveguide, so that the net phase retardation resulting from temperature effects is zero. The structure of fig 16 is thus self-compensating for temperature changes. Another advantage of this structure is that, in a material like lithium niobate, substantially less driving power is needed for a given precision in the conversion. If the field is applied along the c-axis and the incident light is polarized along that axis, then it is calculated from measured values of the electro-optic coefficient that $V_\pi = 2000$ V. Since the field is applied to both waveguides in the interferometer structures (with opposite sign) simultaneously, the appropriate expression for ℓ_π is

$$\ell_\pi = V_\pi \, d/(2V_m);$$

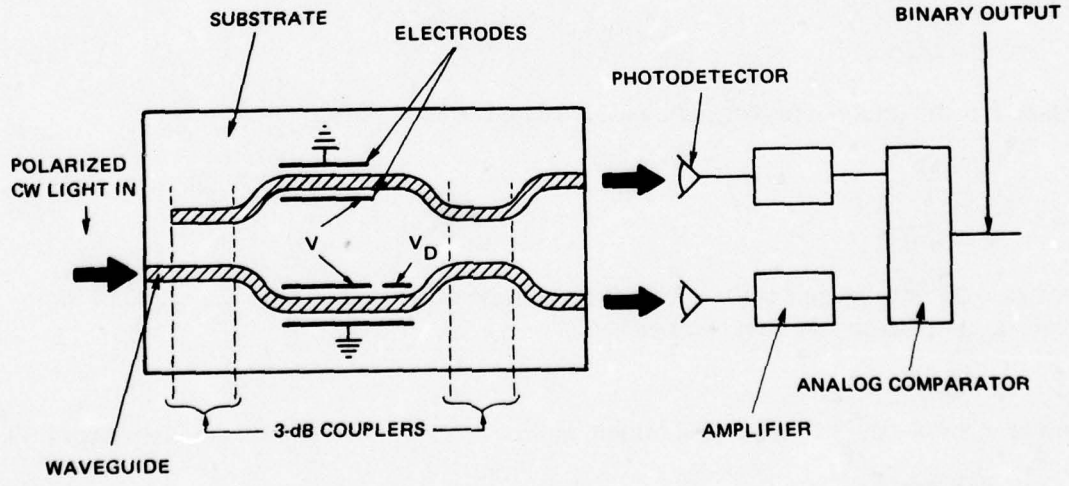

Figure 16. An interferometric modulator for use as a bit channel in the electro-optic A/D converter.

[28]Zernike, F, "Integrated Optics Switch," presented at the OSA/IEEE Topical Meeting on Integrated Optics, New Orleans, La, June 1974

thus, for ℓ_π = 1.08 mm, and ℓ = 1.7 cm, V_m = 4.7 V, compared with 12.5 V in the previous example. This reduction in voltage translates to a significant savings in electrical power, even though the total electrode length, and therefore the capacitance, is twice as great for a given total device length ℓ. From (26), assuming a 500-MHz signal as before, the power is calculated to be only 120 mW, versus 360 mW in the preceding example.

In terms of overall power dissipation, the optical device offers a substantial improvement over conventional A/D converters, primarily because of the reduction in prime power required to drive the comparators. For conversion at a 1-Gb/s sampling rate, it is estimated that the power dissipation is of the order of 0.5 W per comparator. The 64 comparators in an electronic parallel A/D would therefore dissipate 32 watts, versus only 3 watts for the optical device. Assuming 0.3 watt for a laser source, 0.4 watt for the electro-optic portion of the device, and 0.3 watt each for the 12 photodetector/amplifiers raises the total to only 7.3 watts for the optical device.

A limiting factor in implementing fast A/D converters, either electronic or electro-optic, is the speed of the analog comparator. Present commercial devices operate at a rate of less than 4×10^8 comparisons per second, although continuing improvements in high-speed logic devices encourage us to anticipate faster comparators in the near future. Ultimately, the best solution might be to integrate the comparator by fabricating it in the form of an integrated optical logic device on the same electro-optic substrate as the waveguide modulators.

1. ALTERNATIVE TECHNIQUES FOR A/D CONVERSION

The most common method for performing high-speed (>25 megawords/second) A/D conversion is to compare the input voltage V with reference voltages which correspond to different levels in the digital representation of V.[25] This is referred to as the "parallel" method, since all the comparisons are done simultaneously. A three-bit parallel converter is illustrated in figure 17. The reference voltages, which are set by a resistor chain, are each supplied as an input to an analog comparator. The input voltage is supplied through a second resistor chain as the other input to each comparator. The high speed results from the fact that all of the comparisons are done in parallel, but a large number of comparators (2^{N-1} for an N-bit converter) are needed to accomplish this. Furthermore, electronic logic elements are required to convert the comparator outputs to a binary representation of V.

Open-loop successive approximation is a technique for "pipelining" the conversion process by computing the most significant bits first and determining the reference voltage for each subsequent bit from the comparator outputs for previously computed bits. A time delay is required to allow for the computation of the most significant bits before V is applied to the comparators which compute less significant bits. Only N comparators are required with this method, but the synchronization problems are more severe and the time delay between input and output is considerably greater than with the completely parallel approach.

The fastest devices which are commercially available at the present time perform 10^8 conversions/second with 6-8 bits of precision.[29] A device marketed by TRW utilizes two interleaved converters, each of which operates at 5×10^7 conversions/second and utilizes both parallel and serial logic with ECL comparators. The precision is six bits, and the price is $50 000. Other devices with a conversion rate of 10^8/second are available from Biomation

---

[29]Rimmel, AW, "State-of-the-Art Analog-to-Digital Conversion Equipment," Report R-4657, Battelle Columbus Laboratories, Columbus, Ohio, April 1975

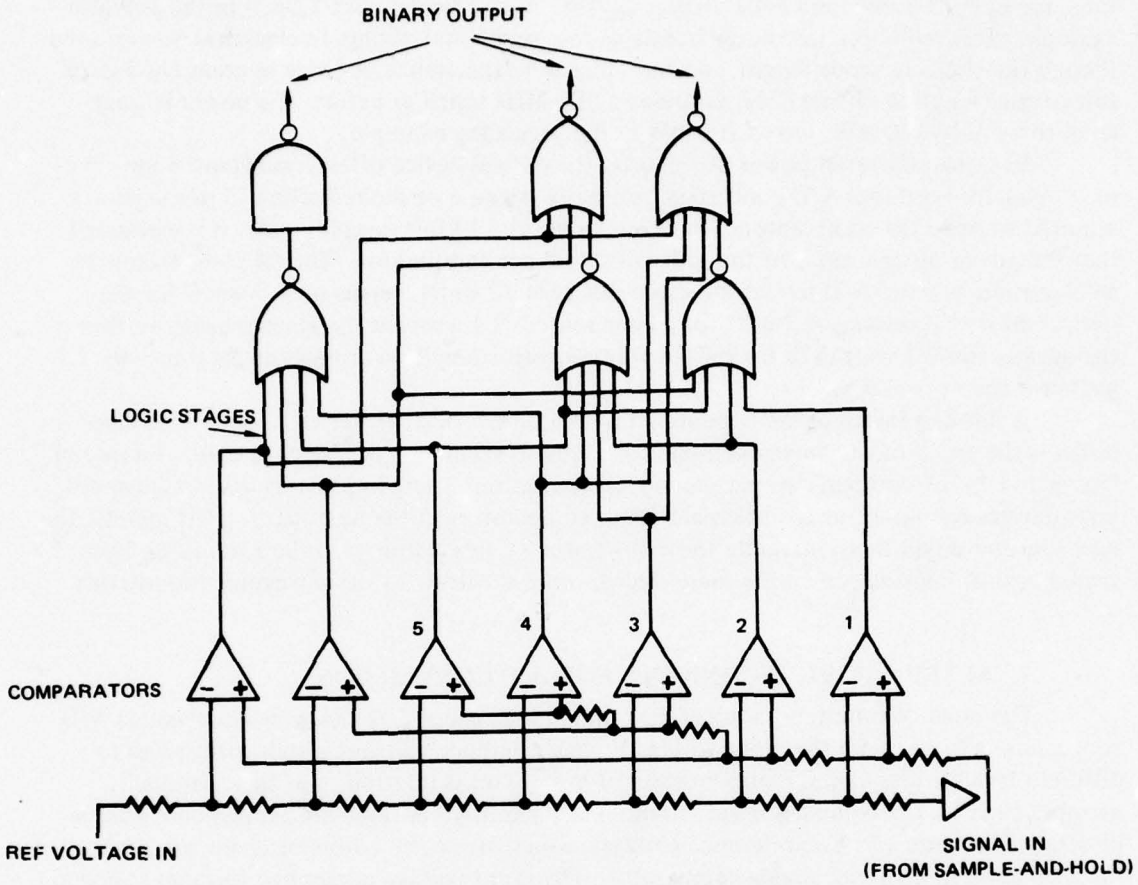

Figure 17. Schematic diagram of an electronic parallel A/D converter with 3 bits of precision.

and from Phoenix, at prices of $9850 and $11 985, respectively. Both use parallel conversion schemes. The Biomation device uses TTL comparators, while the Phoenix Device employs ECL.

Several companies have proposed or are developing devices with conversion rates in excess of 10^8/second.[29] Parallel and successive-approximation schemes using ECL comparators are among the most common approaches. TRW is scheduled to deliver a developmental 5-bit, 400-megaword/second (Mw/s) device to an Air Force sponsor in the near future. A novel technique in which the applied voltage V deflects an electron beam in an electron-bombarded semiconductor device is being pursued by Watkins-Johnson. An electro-optic device which uses a phase grating to deflect a guided light beam has been demonstrated at University College, London.[30] That device is capable of operating at high speeds, but is inherently limited to only 3 bits of precision.

---

[30]Wright, S, Mason, IM, and Wilson, MGF, "High-Speed Electro-optic Analog-to-Digital Conversion," Electron Lett, v 28, p 508-509, November 28, 1974

2. COMPARISON OF ELECTRO-OPTIC A/D CONVERTER WITH PRESENT TECHNIQUES

The electro-optic A/D converter can potentially provide several advantages in comparison with conventional fast parallel A/D converters. First, the number of comparators would be dramatically reduced, from 2^N to N, for an N-bit converter (eg, from 64 to 6 for a 6-bit converter). This would substantially reduce the electrical power drain of the unit (~ 200 mW each for commercial 200-MHz ECL comparators) and would greatly simplify the timing problems which occur in electronic converters because of the large number of comparators.

Another advantage of the optical device is that the use of a repetitively pulsed (mode locked) laser source could eliminate the need for a sample-and-hold device. The function of a sample-and-hold in an A/D converter is to sample the signal at fixed time intervals and maintain the value of the sampled signal during the time a conversion takes place. The output of the sample-and-hold is the voltage input to the device which actually performs the conversion. The drift of the sample-and-hold must be less than $2^{-(N+1)}$ times the full voltage swing to obtain N bits of precision, and the jitter in the sampling clock must be less than $2^{-(N+1)}$ times the conversion period; eg, ~ 8 ps for a 1-gigaword/second (Gw/s), 6-bit converter. With a short optical pulse, the width of the pulse would provide a time window for performing a sampling operation.

Mode-locked argon and Nd:YAG lasers are commercially available, with repetition rates in the hundreds of megahertz, and pulse widths in the 50–200-ps range. (A 50-ps pulse width would be short enough for a 1-gigaword/second, 6-bit converter.) Also promising is the GaAs injection laser, which can be operated on a repetitively pulsed basis. In one case, the pulse width was 200 ps at a repetition rate of 620 MHz.[31] Additional work will be needed to perfect mode-locked injection lasers suitable for use with the optical A/D converter.

A final feature of the optical A/D converter is that the output can be recorded directly upon photographic film. This would make it possible to collect, digitize, and make a permanent record of data at a very high rate. The data could then be processed later at more convenient speeds.

A summary of this section is presented in table 1.

---

[31] Paoli, TL, and Ripper, JE, "Optical Pulses from cw GaAs Injection Lasers," Appl Phys Lett, v 15, p 105-107, August 1, 1969

TABLE 1. HIGH-SPEED ELECTRO-OPTIC A/D CONVERTER – SUMMARY.

Present method: High-speed electronic logic

Elements of integrated optics device:

- Array of modulators on electro-optic substrate
- Injection laser source
- Sample-and-hold interface
- Avalance photodiode detectors
- Electronic comparators.

Potential advantages of integrated optics device:

- Fewer comparators (N versus 2^N)
- No sample-and-hold with pulsed light source
- Lower electrical power dissipation
- Optical output can be recorded directly on film.

Disadvantages:

- Development needed
- Not cost competitive at low (< 25-Mw/s) conversion rates
- Limited to ~8 bits of precision for parallel operation.

Performance-limiting factors:

- Present comparators operate at < 400 MHz
- Commercial avalanche photodiodes limited to ~1 GHz.

Potential performance:

- Near-term (1–3 years) > 400 megaword/second, 6 bits
- Intermediate term (3–6 years) > 1 gigaword/second, 6–8 bits.

Major technology development needed:

- Multichannel modulator fabrication
- Single-mode injection lasers
- Laser-modulator coupling techniques
- Faster comparators
- Mode-locked injection lasers.

B. DELAY-LINE DEVICES

A straightforward application of the optical fiber is for the delay and storage of signals.[32–34] An optical carrier, intensity-modulated by an input signal, is injected into one end of the fiber. An optical receiver at the other end detects and amplifies the light output to

[32]Taylor, HF, Martin, WE, and Caton, WM, "Channel Waveguide Electro-optics Devices for Communications and Signal Processing," presented at the IEEE/OSA Topical Meeting on Integrated Optics, Salt Lake City, January 1976

[33]Wilner, K, and van den Heuvel, AP, "Fiber Optic Delay Lines for Microwave Signal Processing," Proc IEEE, v 64, p 805–807, May 1976

[34]Dillard, GM, Taylor, HF, and Hunt, BR, "Fiber and Integrated Optics Techniques for Radar and Communications Signal Processing," National Telecommunications Conference Record, v III, p 37.5–1 to 37.5-5, December 1976

restore the original signal. The time delay for propagation through the fiber of length L is given approximately by nL/c, where c is the velocity of light in free-space and n is the refractive index of the fiber core. For low-loss silica fibers, the time delay is 4.9 μs per kilometer of length. As indicated earlier, it is possible to produce delay lines with very high (10^5–10^6) time-bandwidth (TB) products using low-loss, single-mode fibers (see fig 12). If the fiber is used for data storage, the number of bits is approximately equal to the TB product. (If the data are injected and detected at the same end of the fiber, with a reflector at the other end, the number of bits is twice the TB product.)

A variable delay line can be produced using segments of optical fiber interconnected through an array of 2 X 2 optical switches, as illustrated in fig 18. Changes in time delay are accomplished by rerouting the signal through fiber segments of different length. If the delay

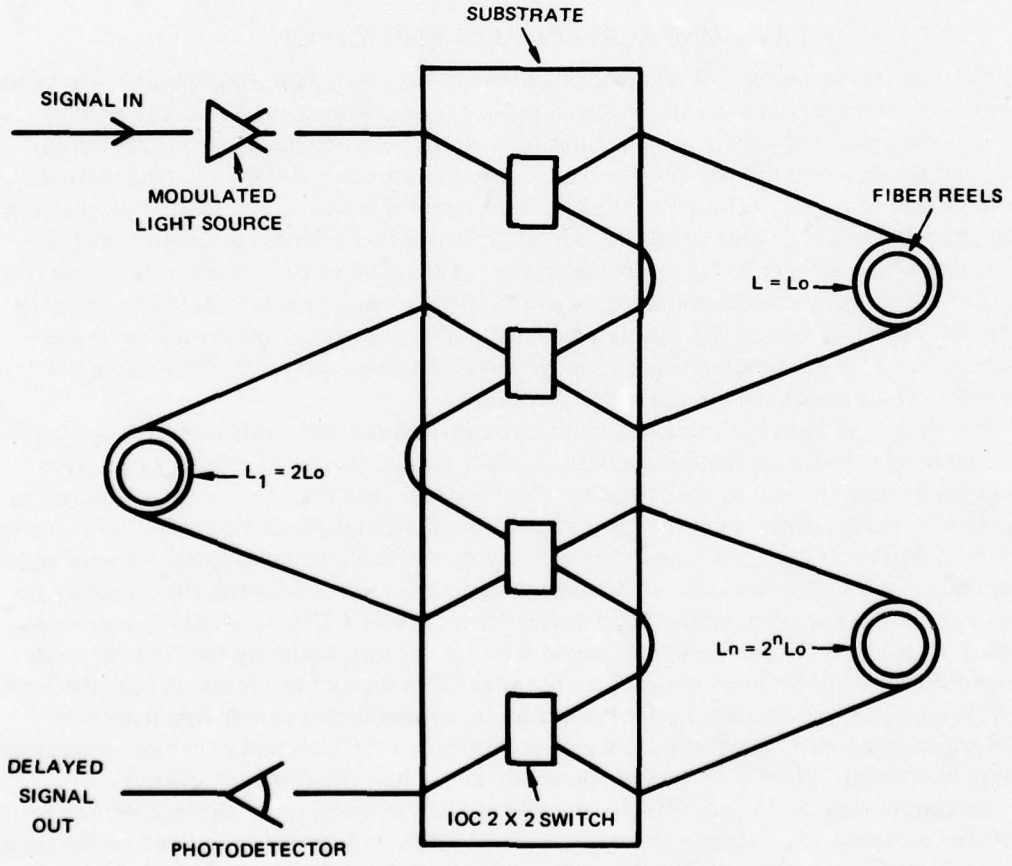

VARIABLE FIBER DELAY LINE

Figure 18. A variable-length fiber optics delay line. Adjacent elements in an array of 2 X 2 electro-optic switches, which could be fabricated on a single substrate, are connected by fibers of different length. The state of each of the switches determines which of the interconnecting fibers transmits the signal to the next switch downstream. The switches can therefore be used to adjust the total length of the delay line.

difference between alternative paths between the nth and $(n + 1)^{st}$ switches is proportional to 2^{n-1}, n = 1,2,3, . . . ,n, then the delay can be programmed to have any of 2^n possible values using only N switches and 2N fibers. Furthermore, the length of the delay line can be changed very rapidly, since the switches themselves operate at high speeds (1-ns switching speed).

It is also possible to implement a tapped delay line using optical fibers. One way of doing this is to inject an input optical signal into a bundle (group) of fibers, each of different length, and detect the signal out to each of the fibers with a single photodetector, as illustrated in fig 19. This represents an optical implementation of the transversal filter, which is used in signal processing for narrowband filters and matched filters. It is also possible to pass the output of each of the fibers through an electro-optic modulator to attenuate the optical output as a means of adjusting the tap weights on a dynamic basis. Finally, as an alternative way of producing a transversal filter, a single fiber can be provided with optical taps along its length, and the accumulated signal from all the taps detected by a single photodetector.

1. SIGNAL DELAY USING SURFACE ACOUSTIC WAVES

Surface acoustic wave (SAW) device technology has emerged during the past few years to provide important new capabilities in signal processing.[35] Functions which can be performed include signal delay, narrowband filtering, correlation, matched filtering, spectrum analysis, and frequency synthesis.[36] The basic configuration for a surface acoustic wave device is illustrated in fig 20. A time-varying electrical signal is fed to an interdigital piezoelectric transducer on the surface of the substrate, which generates two acoustic waves traveling in opposite directions, perpendicular to the electrodes. Almost all of the energy in the wave is confined to within two acoustic wavelengths of the surface. A second interdigital transducer is positioned to receive one of the traveling acoustic waves and transform it back to an electrical signal. An acoustic termination is usually provided to eliminate reflections from the second wave, which is not used in the signal processing.

Quartz and lithium niobate are the most commonly used substrate materials for SAW devices. Metal electrodes are deposited on the surface of a polished and oriented substrate, using photolithographic techniques for pattern delineation. The maximum center frequency and bandwidth are determined by the resolution of the pattern definition process. The center frequency ν_o for the transducer is given by $\nu_o = V_a/\Lambda$, where V_a is the acoustic velocity and Λ is the spatial period of the electrode structure (equal to twice the center-to-center spacing for adjacent electrodes). As an example, for a center frequency of 1 GHz in y-cut lithium niobate (for which $V_a = 3.5 \times 10^5$ cm/s), the electrode width is 0.7 μm, assuming that the electrode widths and the spacings between electrodes are equal. This type of resolution is near the limit of photolithographic capabilities; better resolution to achieve higher center frequencies requires electron beam pattern definition, which is presently a difficult and expensive procedure. Maximum bandwidths in SAW devices are generally about half the center frequency.

Maximum time delay is limited by the size of the substrate, or by signal attenuation. For a 10-cm substrate, the delay for one pass is about 30 μs, but longer delays can be obtained by using reflectors to increase the length of the acoustic path on the chip. At high frequencies, the attenuation is proportional to the square of the frequency; at 1 GHz, for example, the attenuation is 2.5 dB/cm for y-cut lithium niobate and 6.8 dB/cm for y-cut quartz.[37]

---

[35]Slobodnik, AJ, Jr, "Surface Acoustic Waves and SAW Materials," Proc IEEE, v 64, p 581, May 1976

[36]Darby, BJ, "Key Signal Processing Functions Performed with Surface Acoustic Wave Devices," Wave Electronics, v. 2, p 266–290, July 1976

[37]Slobodnik, AJ, "A Review of Material Tradeoffs in the Design of Acoustic Surface Wave Devices at VHF and Microwave Frequencies," IEEE Trans Sonics and Ultrasonics, v SU-20, p 315–323, October 1973

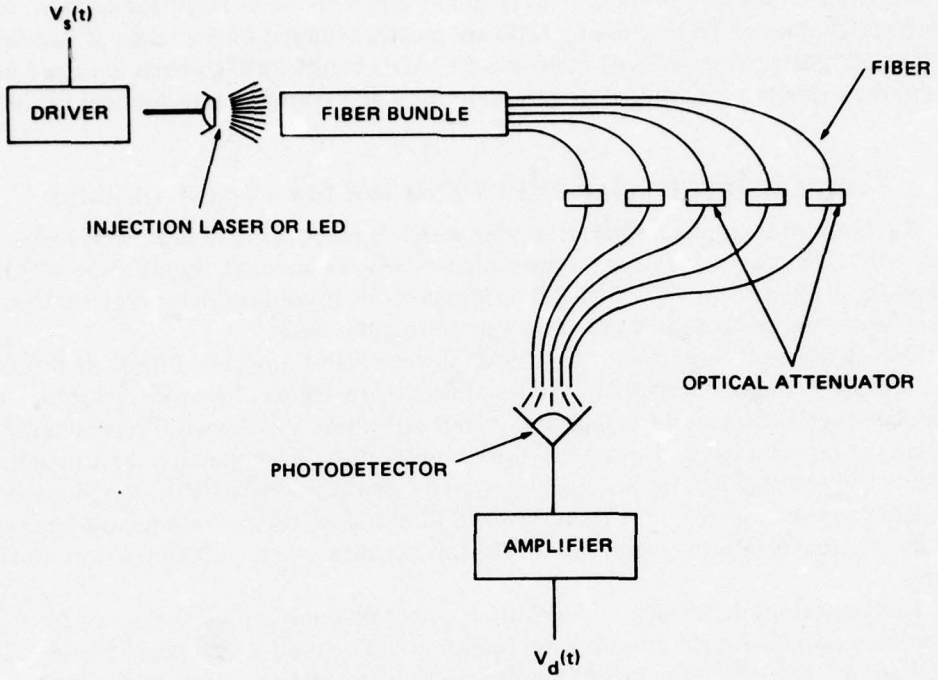

Figure 19. The fiber optics tapped delay line.

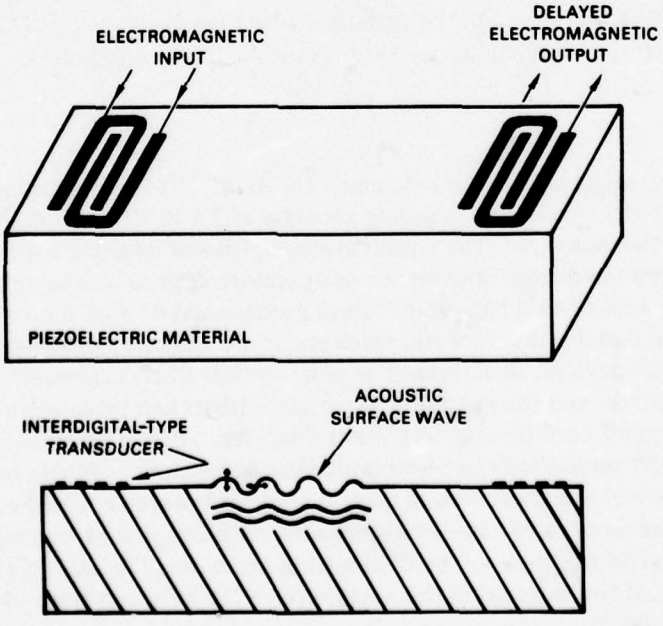

Figure 20. Schematic diagram of a surface acoustic wave (SAW) delay line.

The time-bandwidth product (TB) is an important figure of merit for surface acoustic wave devices. Values of TB of close to 1000 are readily achieved over a range of bandwidths from 10 to 500 MHz, while a TB of 5000 at a 512-MHz bandwidth has been obtained in a lithium niobate device using special pattern definition and fabrication techniques.[36]

2. COMPARISON OF FIBER OPTICS AND SAW DELAY-LINE DEVICES

A feature of the optical fiber delay line which is particularly notable is the high TB product, with calculated values one to two orders of magnitude in excess of those which can be achieved in SAW devices. The high TB products in fibers could allow successive high-resolution radar signals to be integrated on a pulse-to-pulse basis.

One of the most important uses of SAW devices is in transversal filters. If the electrode spacings are equal, the transversal filter passes only narrow bands of frequencies centered at harmonics of the fundamental frequency ν_0. Matched filters and shaped filters are produced by varying the tap spacings and weights. A desirable feature is programmability, in which the tap weights and spacings can be switched by external control signals. Only very limited programmability is now available in SAW transversal filters, since the switching must be accomplished by external electronic circuitry and the tap spacings are essentially fixed by the device structure.

This important deficiency of SAW filters might be remedied by the use of fiber optics and integrated optics. An electro-optic modulator could be used to attenuate the signal input to each fiber as a means of rapidly varying the tap weights, and each fiber in the filter could be replaced by a variable delay line of fig 18. This would provide a means for rapidly reconfiguring both the tap weights and spacings of the filter. The uses of such a "programmable fiber optics transversal filter" (PFOTF) are discussed in section IV, "Applications."

The change in delay time as a result of ambient temperature variations is an important problem in some SAW devices, and the materials with high electroacoustic constants are those most sensitive to temperature changes. As an example, the temperature coefficient of delay

$$\frac{1}{\tau}\left(\frac{d\tau}{dT}\right)$$

is $9.4 \times 10^{-5}/°C$ in y-cut lithium niobate and $-2.4 \times 10^{-5}/°C$ in y-cut quartz, at room temperature, while the electroacoustic coupling constant is 2.4×10^{-2} for the lithium niobate and 9×10^{-4} for the quartz.[37] The temperature coefficient of delay for light transmission in fused silica, as determined from data on the temperature dependence of refractive index,[38] is $1.1 \times 10^{-5}/°C$, or 12% of that for y-cut lithium niobate and 45% of the value for y-cut quartz.

The optical signal generators and receivers have a fan-out and fan-in capability not matched by acoustic devices. A thousand or more optical fibers can receive the signal from a modulated light source, and the output of these same fibers can be coupled to a single photodetector (a commercial fiber bundle with 2000 fibers has a diameter of less than 4 mm, quite compatible with PIN photodiode or photomultiplier dimensions). Furthermore, it is possible to perform multisensor signal processing using one optical source coupled to a bundle of fibers for each sensor. Similarly, an array of photodiodes, each coupled to a group of fibers, could be provided. These possibilities will be discussed in more detail in section IV.

Summaries of the material in this section on delay lines and transversal filters are presented in tables 2 and 3.

---

[38]Wray, JH, and Neu, JT, "Refractive Index of Several Glasses as a Function of Wavelength and Temperature," J Opt Soc Amer, v 59, p 774–776, June 1969

TABLE 2. HIGH TIME-BANDWIDTH FIBER OPTICS DELAY LINES – SUMMARY

Present method: Surface acoustic wave (SAW) devices.

Elements of device:

Laser source (current-modulated)
Long single-mode fiber
Photodetector
Repeater (for recirculation)
Switch (for programmability).

Potential advantages of fiber/integrated optics device:

High time-bandwidth product (10^5–10^6 versus 10^3 @ 1 GHz).

Disadvantages:

High cost ($1–$10/m) for present low-loss fibers.

Performance-limiting factors:

Fiber attenuation limits maximum delay time
(~ 100 μs for 2-dB/km attenuation).

Potential performance:

Near-term (1–3 years): 200 μs @ 500 MHz
Intermediate term (3–6 years): 500 μs @ 1 GHz.

Risk factors:

Continued high fiber cost

Major technology development needed:

Manufacturing techniques for very-low-loss, single-mode fibers
Wideband repeater for recirculator.

TABLE 3. FIBER OPTICS TRANSVERSAL FILTERS – SUMMARY

Present method: Surface acoustic wave (SAW) devices.

Elements of device:

- Injection laser source
- Bundle (group) of optical fibers cut to different lengths
- Electro-optic switches and modulators (for programmability)
- Photodetector.

Potential advantages of fiber/integrated optics device:

- Programmability of tap weights and spacings
- Large number of taps (> 500)
- Large number of delay lines per signal source (> 500)
- Low temperature coefficient of delay (12% of that of SAW in y-cut lithium niobate)
- Precise control of tap spacings (0.01 ns versus 2–5 ns)
- Low cost for complex filters and correlators.

Disadvantages:

- Generally not cost-competitive for narrowband rf filters and some matched filters
- Some technology development needed.

Performance-limiting factors:

- Present modulators and commercial avalanche photodiodes limited to $\sim$1 GHz.

Potential performance:

- Near-term (1–3 years): 500 taps, 1 GHz
- Intermediate term (3–6 years): > 1000 taps, > 1 GHz.

Major technology development needed:

- Switch for programmable delay line
- Improved techniques for connecting fibers to injection laser sources and to waveguides.

C. PSEUDORANDOM SEQUENCE GENERATOR

Pseudorandom binary sequences have a variety of applications in radar and communication systems.* (These sequences are also referred to as m-sequences, maximal-length sequences, and direct sequences.) The applications include generation of radar signals having high range resolution, low peak power, and long time duration;[39] techniques for spread-spectrum communications;[40] and coding for secure communication. Generation of these sequences digitally is restricted by the speed of operation of the digital logic devices (shift registers, gates, etc.), and by propagation delays associated with feedback from one register stage to another. As a result, sequence generators requiring both high speed and extremely long shift registers are impractical.

An electro-optical generator of direct sequences is described.[34] It is shown that sequences of length 2^{N-1} can be generated using the equivalent of an N stage shift register with feedback. However, the speed of the digital circuits is far exceeded since very narrow pulses can be transmitted through fiber optics delay lines, detected, and retransmitted. Since propagation delay is used in producing the binary sequences, it is not a limiting factor in the speed of operation. Also, the equivalent number of shift-register stages can be very large (500 or more), thus providing extremely long cycle times even at gigabit/second (Gb/s) rates.

The properties of shift-register sequence generators are not discussed here since several references discuss in detail both the theory and implementation of these generators. See footnote.

The direct sequence generator is illustrated schematically in fig 21. A mode-locked laser emits very narrow light pulses at a fixed rate R=c/2L, where c is the velocity of light and L is the laser cavity length. Pulse widths can be 50 ps or shorter, and typical pulse repetition rates are several hundred megahertz. The repetition rate can be increased by multiples of the fundamental using a beam-splitter/combiner external to the laser cavity. The optical parity generator (OPG) is a device which passes the laser light pulse only if a voltage V is applied to an odd number of electrodes. (The OPG is described at the end of this section.) The light pulses passed by the OPG are propagated through N fibers, which have delays T, 2T, . . . ,NT, where T=1/R is the time between laser pulses. (Actually, the total delay, including the delay through the photodetector and the electrical delay through the switch to the electrode, is a multiple of T.) The code selection switches are used to determine which "feedback taps" are used for generating the direct sequence. If a switch is closed, a pulse of voltage V is applied to the corresponding electrode when a light pulse is applied to the input of the photodetector; if a switch is open, the electrode is at ground level. Because of the choice of total delay in the fibers, the voltage pulse is made to appear at the electrode at the time that the laser emits a pulse. The output from the OPG is thus controlled by the appropriate outputs from the fibers and a direct sequence is generated.

Electrode E_0 is used to enter an initial value into the generator when all of the code selection switches are open. Once the initial conditions have been entered, E_0 is set to ground and the appropriate code selection switches are closed. Figure 22 shows the sequence of

---

*There are myriads of papers, books, and articles on the subject of pseudorandom binary sequences; however, to conserve space, only two are referenced here. Chapter 4, Part IV of Berkowitz (39), written by M. P. Ristenbatt, and Chapter 3 of Dixon (40) contain a complete discussion of sequence generation and applications and also list several references.

[39] Berkowitz, RS, "Modern Radar," Wiley, New York, 1965

[40] Dixon, RC, "Spread Spectrum Systems," Wiley, New York, 1976

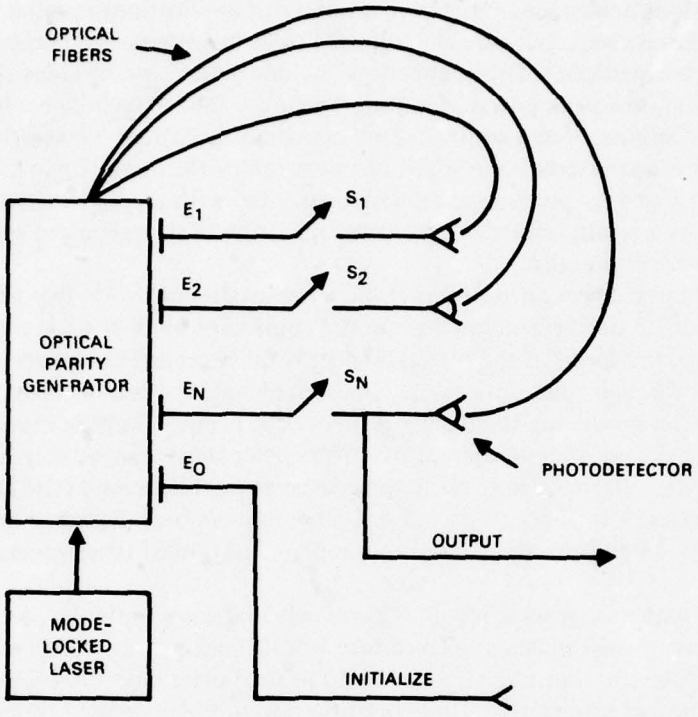

Figure 21. Optical generator of direct sequences.

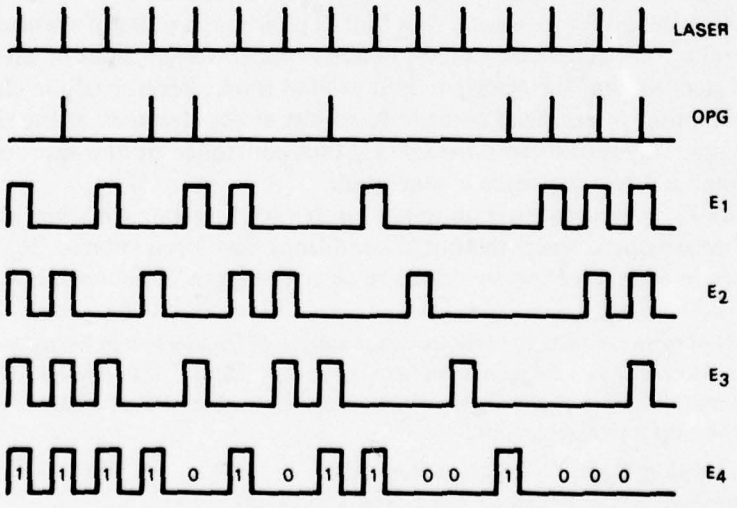

Figure 22. Output sequence from optical direct-sequence generator.

pulses generated for the case where N = 4 and switches S_1 and S_4 are closed, with the initial condition 1111. (That is, the equivalent 4-stage shift register would begin with all stages at "1".)

Two direct sequences of different lengths, 2^{N-1} and 2^{M-1}, can be modulo-two added to produce a composite sequence of length $(2^{N-1})(2^{M-1})$.[38] Similarly, if two direct sequences of the same length are modulo-two added, the result is a so-called Gold code.[38] The modulo-two addition of two or more direct sequences, each generated electro-optically, can also be performed electro-optically, as shown in fig 23. The output from each optical direct sequence generator is an input to an electrode of an OPG which uses a mode-locked laser with the same cavity length (and, hence, the same pulse rate) as is used in each of the sequence generators. The photodetected output from the OPG is the modulo-two sum of the input sequences. Also shown in fig 23 is a data input to the OPG. For spread-spectrum communications application, a direct sequence is modulo-two added to the data stream and the resulting sequence controls the modulation of the carrier; eg, biphase modulation determined by a binary sequence. Thus, the combiner shown in fig 23 can add direct sequences to increase the sequence length, and can combine data and direct sequences.

The OPG is shown schematically in fig 24. A single-mode waveguide branching structure[16,17] is fabricated in a linear (Pockels) electro-optic material[15]. Light from a cw or mode-locked laser source is coupled into the initial waveguide. The total phase retardation of light which propagates through one arm of the branch with respect to that which propagates through the other arm is given by $\Delta\Gamma = n\pi$, where n is the number of signal electrodes which are activated with a voltage of appropriate magnitude, here taken to be V_o (that is, $V = V_o$ for a "1" and V = 0 for a "0"). The optical intensity output of the branching modulator structure is given by $I_o = A \cos^2(\Delta\Gamma/2) + B$, where A and B are positive constants, and the sum of A and B is proportional to the incident optical intensity. Therefore, $I_o = B$ if the input signals have odd parity, and $I_o = A + B$ if the signals have even parity. (With proper design, it is expected that $B/A \ll 1$.)

The conventional method for generating pseudorandom binary sequences utilizes a binary shift register with feedback from various register states. Logic elements (flip-flops, gates, etc) have been produced so that the sequences can be generated up to 300-Mb/s rates. However, because of propagation delay, the number of shift-register stages is limited, and thus the cycle time is also limited. (The cycle time of a "linear" shift-register sequence generator is always less than $R(2^{N-1})$, where R is the rate at which the register is shifted and N is the total number of shift-register stages.) The maximum bit rate of a shift-register sequence generator is determined not only by the switching rate of the shift-register stages but also by the propagation delay in its feedback network. The bit rate is thus less than or equal to $R_{max} = 1/(T_R + T_M)$, where T_R is the time for a shift-register stage to reach its next state and T_M is the propagation delay. Seven-stage shift-register generators utilizing ECL (emitter-coupled logic) elements capable of operating in excess of 200 Mb/s have been implemented; however, extending the length of the register to generate a more useful (longer cycle time) sequence would slow the code rate significantly. Thus, the limitations and disadvantages of current methods of generating pseudorandom binary sequence include the following: (a) the bit rate is limited to about 300 Mb/s for a short sequence, and is even less for longer sequences; (b) the register length for a given rate is limited by propagation delay; and (c) high-speed logic devices generally require high current and thus dissipate large amounts of heat when operating at high speeds.

A summary of the material presented in this section is included in table 4.

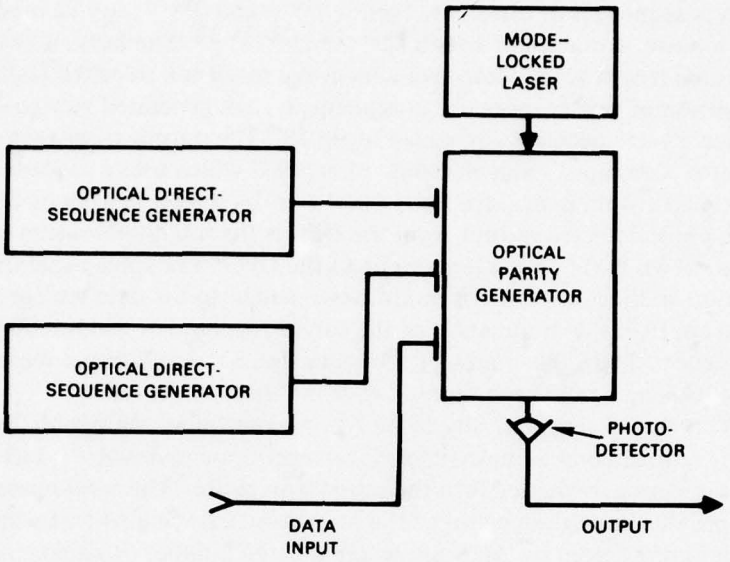

Figure 23. Electro-optically combining direct sequences.

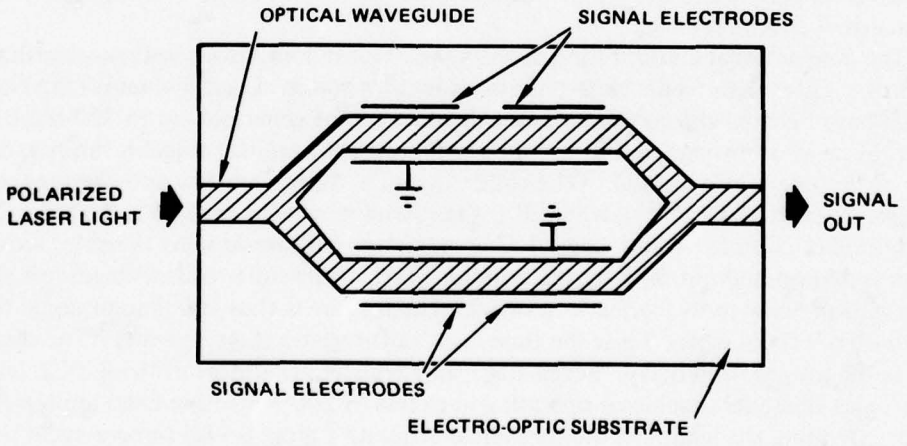

Figure 24. The optical parity generator.

TABLE 4. OPTICAL PSEUDORANDOM SEQUENCE GENERATOR – SUMMARY

Present method: Digital shift registers.

Elements of device:

- Laser source
- Fiber bundle (group)
- Photodetector/amplifiers
- Electro-optic modulator (parity generator).

Potential advantages of fiber/integrated optics device:

- High generation rate (> 1 GHz)
- Low electrical power dissipation
- Low cost.

Disadvantages:

- Not presently available.

Performance-limiting factors:

- Present modulators (parity generators) and commercial avalanche photodiodes limited to ~1 GHz.

Potential performance:

- Near-term (1–3 years); $2^{50}-1$, 1 Gb/s
- Intermediate term (3–6 years): $2^{100}-1$, 3 Gb/s.

Major technology developments needed:

- Wideband repeater
- Optical parity generator.

D. BRAGG CELL SPECTRUM ANALYZER

The Bragg acousto-optic modulator can be used as a wideband spectrum analyzer for electrical signals. Such a device is illustrated schematically in fig 25. The incoming signal is applied to the electrodes of an electro-acoustic transducer, which launches a traveling acoustic wave into the material. This acoustic wave deflects part of the light in a collimated beam from a laser source. The light emerging from the material is collected and focused by a lens. If only one frequency component is present in the modulating signal, two spots will appear in the focal plane of the lens, one corresponding to the undeflected (zeroth order) beam, the other corresponding to the deflected beam. The displacement of the deflected beam spot is close to a linear function of frequency, and if more than one frequency is present in the beam, a spot corresponding to each will appear. Wideband signals will produce a line in the focal plane of the lens.

The focused output of the Bragg cell can be recorded on moving photographic film, to give a plot of the spectrum as a function of time, or can be detected by elements in a

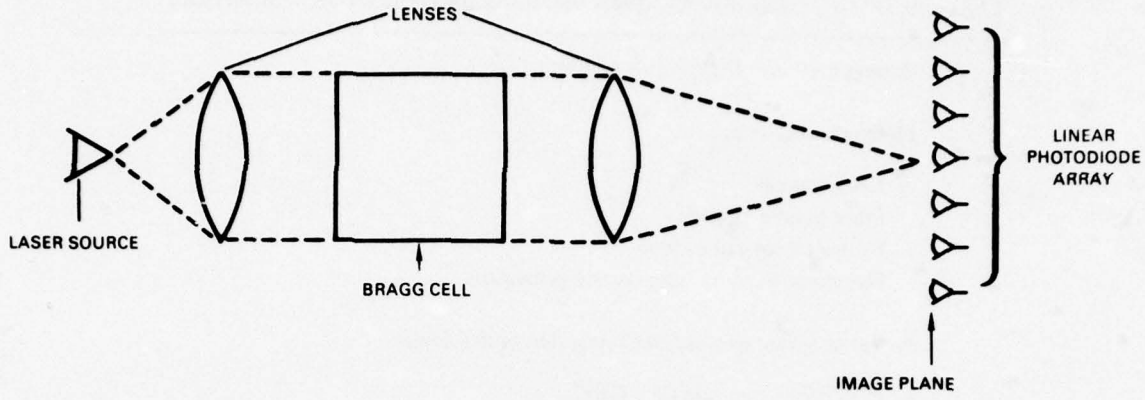

Figure 25. Schematic diagram of a Bragg cell spectrum analyzer.

photodiode array. In the latter case, each photodiode in the array represents one resolution element in the rf spectrum of the incoming signal. The present practice is to use a self-scanned array of the type found in vidicons. The cost of such an array is much lower (~ $2000 for a 512 X 1 array) than for an equal number of discrete photodiodes and amplifiers. Unfortunately, noise introduced during the array scanning process causes considerable degradation of the electrical output signal.

Thin-film versions of the Bragg cell spectrum analyzer also have been fabricated in the laboratory.[13] One of these devices used lithium niobate as the substrate material and out-diffusion to produce the waveguide. A set of four tilted transducers, each tuned to a different center frequency, was employed to obtain wideband (~ 350 MHz) operation.

In comparison with the bulk device, the thin-film Bragg cell spectrum analyzer offers the potential for operating with considerably reduced rf drive power. This is true because the diffraction efficiency in either case is proportional to the acoustic power density averaged over the region of optical propagation. In the surface wave case, both the optical and acoustic waves are confined within a few micrometres of the surface, while in the bulk device the height H of the optical beam, measured perpendicular to the surface, is determined by diffraction effects and has a minimum value of $h \sim 10\lambda d/n$, where λ is the optical wavelength in the material, d is the length of the acousto-optic interaction region, and n is the refractive index of the material. The ratio of acoustic power in the bulk case P_b to that for the surface wave device P_s is

$$P_b/P_s \sim h/\Lambda ,$$

where Λ is the acoustic wavelength. As an example, if $\lambda = 0.63\ \mu m$, d = 1 cm, and n = 2.0, then $h \sim 600\ \mu m$. For the acoustic wave at a frequency of 500 MHz, $\Lambda \sim 7\ \mu m$. In this example,

$$P_b/P_s \sim 85 = 19.2\ dB .$$

However, a simple comparison of acoustic powers does not take into account the transducer efficiencies and selection of materials in the two cases. Both of these factors favor the bulk device, at least at the present state of the technologies. The loss in converting from electrical to acoustic power is, typically, 5–15 dB for surface wave transducers and 2–5 dB for bulk transducers. The bulk device offers considerably more flexibility with regard to

choice of materials because in the bulk case there is no requirement that low-loss optical waveguides be fabricated in the material. Optical waveguides with low loss (say < 3 dB/cm) have been produced in relatively few acousto-optic materials (ZnSe, CdS, $LiNbO_3$), and none of these has as high an acousto-optic figure of merit as TeO_2, which is commonly used for bulk modulators. Lithium niobate, the substrate most commonly used for surface-wave modulators, requires 12 dB more acoustic power to provide a given beam deflection than does TeO_2. However, there is apparently no reason to believe that low-loss modulators cannot be made in TeO_2.

Although surface-wave modulators have the potential for considerable improvement over bulk devices in drive power, the same cannot be said with regard to frequency of operation. Presently, the technology for producing very wideband (500 MHz – 1 GHz bandwidth) transducers for bulk waves is considerably ahead of the corresponding capability in the surface-wave area. Acousto-optic spectrum analyzers with 1-GHz bandwidth have been produced in bulk Bragg cells, while the maximum bandwidth which has been achieved with surface wave Bragg cells (using four transducers) is less than 400 MHz.

A summary of the material in this section is presented in table 5.

TABLE 5. INTEGRATED OPTICAL BRAGG CELL SPECTRUM ANALYZER – SUMMARY

Present method: Bulk Bragg cell device.

Elements of integrated optics device:

- Laser source
- Acousto-optic Bragg cell beam deflector
- Photodetector array.

Potential advantages of integrated optics device:

- Lower rf drive power
- Size reduction
- Lower cost.

Disadvantages:

- Substantial amount of technology development needed.
- Very high bandwidth (> 500 MHz) more readily achieved in bulk device.
- Selection of acousto-optic materials limited to those in which low-loss waveguides can be fabricated.

Performance-limiting factors:

- Bandwidth limited by surface-wave transducer technology
- Resolution limited by acoustic attenuation and size of substrate
- Dynamic range limited by photodetector noise and light scattering.

Potential performance:

- Near-term (1–3 years): 500 MHz, 500-kHz resolution, 50-dB dynamic range
- Intermediate term (3–6 years): 1 GHz, 500-kHz resolution, 60-dB dynamic range.

Major technology development needed:

- *Single-transverse-mode injection lasers
- *Low-noise photodiode arrays
- Fabrication techniques for integrated waveguide/lens
- Fabrication of waveguides in TeO_2 or comparable materials.

*Needed to improve dynamic range of both bulk and integrated optics device.

E. SWITCHED NETWORK

Optical networks can, in principle, be made up of 2 × 2 electro-optic switches, such as the one illustrated in fig 9, interconnected by dielectric waveguides on a single substrate.[41,42] This section considers optical implementation of the N × N rearrangeable connecting network[43] in which, by a suitable choice of the states of individual switches, any combination of one-to-one links between N input and N output terminals can be established.

A number of analyses directed toward minimizing the number of switches and stages in connecting networks have been carried out.[43] These analyses generally have assumed that crossings between transmission paths which interconnect the switches are allowed. However, the fabrication of optical networks with crossing interconnections on a single substrate may prove difficult. No techniques for crossing one channel waveguide above another have yet been demonstrated. An alternative would be for the crossing waveguides to intersect one another, but this would introduce loss and crosstalk if the angle between waveguides were small. The attainment of large-angle intersections would require sharp bends, which, again, would cause excessive loss. Accordingly, the following discussion deals with networks with no crossings, of the type illustrated in fig 26.

The signal flow in a network can be described by indicating which waveguide carries each signal in each network stage. This information is provided for an N × N network with m switching stages by a function $\pi_j(I)$; π, I, and j are integers; $1 \leqslant \pi \leqslant N$, $1 \leqslant I \leqslant N$, $0 \leqslant j \leqslant m$. The integers π, I, and j identify, respectively, the waveguides, signals, and network stages. No two signals can occupy the same waveguide in the same stage; that is, $\pi_j(I) = \pi_j(I')$ only if $I = I'$. The input and output signal distributions, $\pi_0(I)$ and $\pi_m(I)$, $1 \leqslant I \leqslant N$, are assumed to be given; this specifies the input-to-output link assignment. A switching algorithm determines the states of the switches which complete a given link

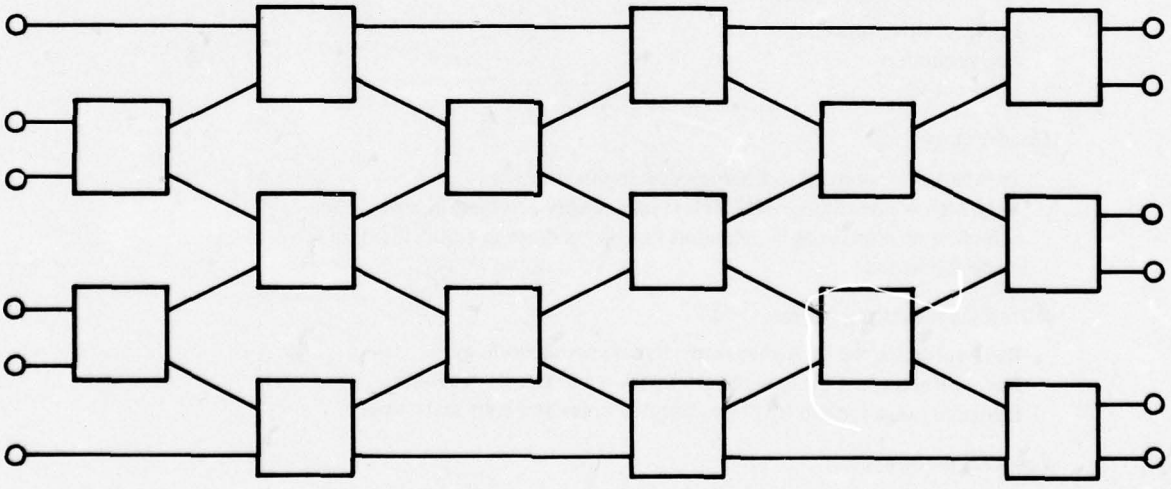

Figure 26. A 6 × 6 connecting network consisting of 2 × 2 optical switches interconnected by single-mode dielectric waveguides on a single substrate.

[41] Taylor, HF, "Optical Waveguide Connecting Networks," Electron Lett, v 10, p 41-43, February 28, 1974

[42] Soref, RA, "Optical Switch Study," TR 75-3, Rome Air Development Center, Rome, N Y, February 1975

[43] Benes, VE, Mathematical Theory of Connecting Networks, Academic Press, New York, 1965

assignment. In the case of the noncrossing network, an efficient algorithm requires that the state of each switch be chosen to be such that its output signals are in the same relative position in the waveguide matrix that they are required to occupy in the final (output) stage. More formally, if the signals I and I′ are incident on a switch in adjacent waveguides in the j^{th} stage, then $\pi_{j+1}(I) = \pi_{j+1}(I') + 1$ if $\pi_m(I) > \pi_m(I')$, and $\pi_{j+1}(I) = \pi_{j+1}(I') - 1$ if $\pi_m(I) < \pi_m(I')$. An illustration of signal flow in the 6 × 6 network of fig 26 resulting from the application of this algorithm is given in table 6. In this example, the link assignment requires that the network reverse the order of signals in the waveguide matrix. This network, with 15 switches and six switching stages, can implement any link assignment for six inputs and outputs. More generally, an N × N network of this type requires N(N−1)/2 switches and N switching stages for $N \geq 3$. An N × N network with crossed interconnections requires a minimum of

$$N\langle \log_2 N\rangle - 2^{\langle \log_2 N\rangle} + 1$$

switches,[44] where ⟨J⟩ denotes the least integer greater than or equal to J. The 6 × 6 network with crossed interconnections, for instance, requires 11 switches.

Integrated optics devices used in conjunction with single-mode fibers represent an attractive alternative for future implementation of high-data-rate computer communications networks. Several advantages of the optical approach in comparison with electronic switching are apparent. (1) The data transmission capacity of an electronic switch is limited by the switching speed of the digital logic family used for implementation (eg, 25 Mb/s for TTL, 250 Mb/s for ECL/10 000). The data rate which can be handled by an optical switch is in the tens of gigahertz and is independent of the electronic control circuitry. (2) The electrical power requirement per switching operation is roughly the same for electronic and integrated optical switches (eg, 10–50 pJ/cycle). However, changes in state of the electronic switch are governed by the transmitted data rate, while changes in state for the optical switch are governed by the switching rate, which is typically two or three orders of magnitude lower

TABLE 6. SIGNAL FLOW IN A 6 × 6 NETWORK. VALUES OF I ARE TABULATED FOR THE INPUT-OUTPUT LINK ASSIGNMENT

$\pi_0(I) = I$, $\pi_6(I) = 7 - I$.

π \ j	0	1	2	3	4	5	6
1	1	2	2	4	4	6	6
2	2	1	4	2	6	4	5
3	3	4	1	6	2	5	4
4	4	3	6	1	5	2	3
5	5	6	3	5	1	3	2
6	6	5	5	3	3	1	1

[44]Joel, AL, "On Permutation Switching Networks," Bell Syst Tech J, v 47, p 813-822, May-June 1968

than the data rate. The overall power dissipation in the device material, which is an important factor in determining element packing density, size, and data capacity of a large switch, is therefore expected to be much lower using integrated optics technology. (3) Microwave signal radiation and pickup, which cause extremely severe crosstalk problems in high-data-rate, high-density electronic switches, are eliminated by the use of an optical carrier. (4) The prospects for large-scale integration (eg, 1000–10 000 switches on a 5-cm × 5-cm substrate) are evidently much better with an integrated optics switch than with ECL technology, particularly in view of the signal radiation problem in the latter case.

A summary of the information in this section is presented in table 7.

TABLE 7. HIGH-SPEED ELECTRO-OPTIC SWITCH – SUMMARY.

Present method: Electronic logic (ECL, TTL).

Elements of integrated optics device:

- Network of 2 × 2 switches on electro-optic substrate
- Optical fiber interconnections
- Electronic control circuitry.

Potential advantages of integrated optics:

- High throughput data rate (>1 Gb/s)
- Large number of input-output terminals (> 100 × 100)
- Low electrical power dissipation
- Immunity from signal interference
- Amenable to large-scale integration (> 1000/cm^2).

Disadvantages:

- Considerable technology development needed.

Performance-limiting factors:

- Switch crosstalk (-26 dB demonstrated in lab)
- Packing density limited by electrical contacts (~ 1000/cm^2).

Potential performance:

- Near-term (1-3 years): 20 × 20, 10-ns switching speed, 1-Gb/s data rate
- Intermediate term (3-6 years): 100 × 100, 10-ns switching speed, > 1-Gb/s data rate.

Major technology development needed:

- Crosstalk reduction in 2 × 2 switches
- Techniques for large-scale integration of switching elements.

IV. APPLICATIONS

This section discusses potential applications of fiber optics and integrated optics for signal processing in radar, electronic warfare (EW), communications and multisensor data collection systems.

A. RADAR

Several of the signal-processing functions required by radar systems can be implemented with fiber and integrated optics components. In some cases, it appears that these components provide a means for significant improvement in performance compared with current signal-processing techniques. In fact, some techniques which are impossible (or impractical) to implement with conventional hardware are made possible (and practical) by fiber and integrated optics devices. Radar applications of fiber and integrated optics are discussed below.

1. DELAY LINES FOR PULSE-TO-PULSE INTEGRATION

Radar detection of targets in clutter generally can be improved by reducing the range-cell size (increasing the range resolution) to the point where the total amount of clutter within one range cell is much smaller than the target cross section. Thus, when the targets to be detected are small, such as floating logs, oil drums, etc, the signal bandwidth is very large (approximately 500 MHz for 1-foot resolution). One would be especially concerned with detection of small floating objects in connection with the operation of high-speed craft, such as hydrofoils and surface-effect ships. Additional clutter suppression can be achieved by pulse-to-pulse integration of the radar returns; however, for this integration to be most effective requires that the resolution properties of the signal be preserved. The gain in signal-to-clutter ratio that can be achieved by integration is illustrated pictorially in fig 27.

Pulse-to-pulse integration of wideband radar returns generally has not been feasible because there has been no technique for storing wideband (500 MHz) signals for long (approximately 200 μs) interpulse periods. Delay lines with 500-MHz bandwidth are presently available (folded-tape meander line, YIG crystal, etc), but the maximum delay at this bandwidth is only a few μs. Time delays of hundreds of μs can be achieved in surface acoustic wave (SAW) delay lines, but the bandwidths achievable for delays greater than 50 μs are much less than 500 MHz. However, fiber optics delay lines can be used to store wideband signals, and integration of high-resolution radar returns on a pulse-to-pulse basis can be performed electro-optically.

One method for performing pulse-to-pulse integration is shown in fig 28. The output from a laser is electro-optically modulated by the wideband radar video and propagated through a fiber optics delay line. The output from the fiber is photodetected, amplified, and used to modulate the input to another fiber optics delay line, as shown in the figure. The total delay through the modulator, fiber, photodetector, and amplifier combination is matched to the interpulse period so that returns from the same range cell appear at the amplifier outputs at the same time and are (noncoherently) integrated.

A simpler method for performing pulse-to-pulse integration is shown in fig 29, and involves only one fiber optics delay line. In this implementation, the sum of the radar video $V_R(t)$ and the delayed signal $V_D(t)$ are used to modulate the optical input to the fiber optics delay line. The output from the fiber is photodetected, amplified, and summed with the input radar video $V_R(t)$. The total delay is matched to the interpulse period, and the amplifier

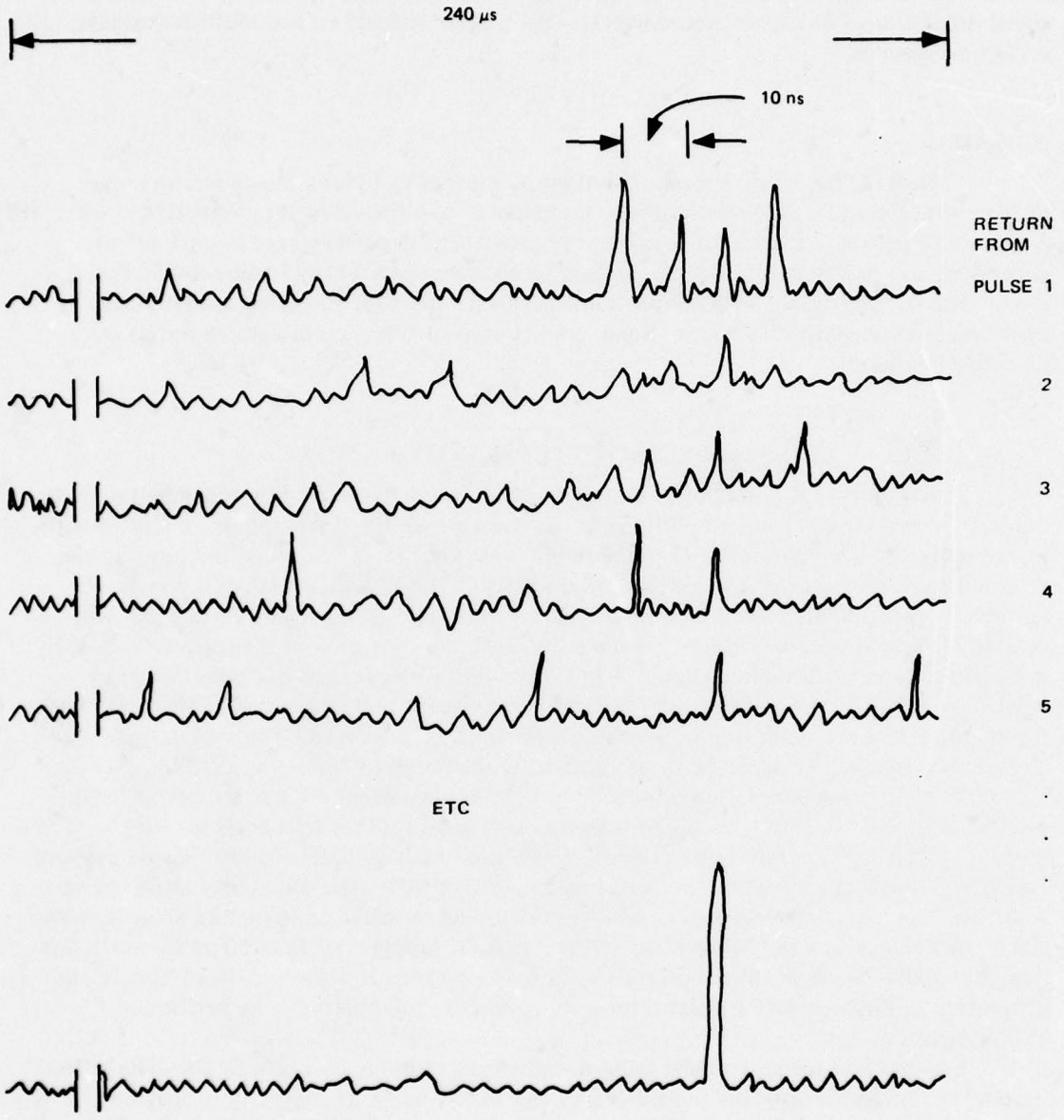

Figure 27. Pulse-to-pulse integration for clutter suppression in a high-resolution radar.

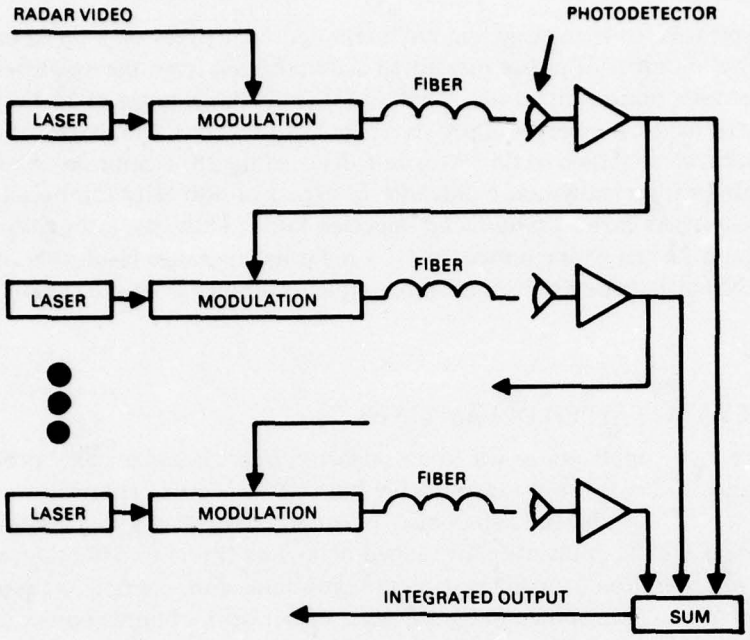

Figure 28. Electro-optical pulse-to-pulse integration of high-resolution radar returns.

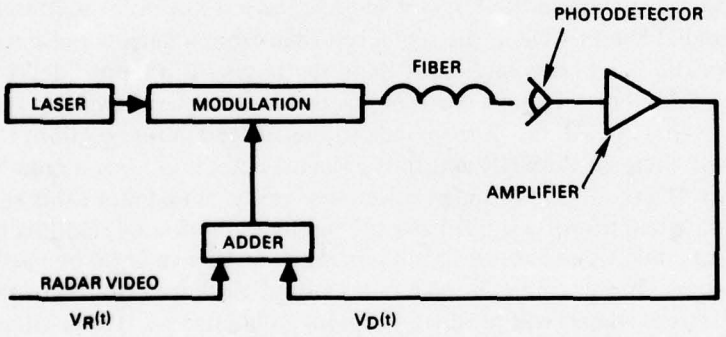

Figure 29. Recursive electro-optical integration of high-resolution radar returns.

djusted so that the total gain G is less than unity. Returns from a specified range cell after k^{th} pulse will appear at the adder input at times $t_o + kT$, where t_o is measured from the e of transmission of each radar pulse, and T is the interpulse period. For this range cell, amplifier output $V_D(t_o + nT)$ after the n^{th} pulse can be written as:

$$V_D(t_o + nT) = \sum_{k=0}^{n-1} V_R(t_o + kT)G^{n-k}$$

$$n = 1,2, \ldots,$$

Thus, the radar returns for each range bin are integrated recursively on a pulse-to-pulse basis, and the "effective" number of pulses integrated is determined from the amplifier gain G.[45]

The interpulse period for a radar having an unambiguous range of 18 kilometres (approximately 10 nautical miles) is approximately 125 μs. Thus, the length of fiber needed to implement the system shown in fig 29 (or one delay in fig 28) is approximately 25 km. The data presented earlier show that bandwidth in excess of 500 MHz can be achieved at this length using a (Ga,Al)As current-modulated injection laser. Thus, the integration schemes of both figures 28 and 29 can be implemented for a radar having range resolution of approximately 1 foot (500-MHz bandwidth) and an unambiguous range of approximately 10 nautical miles.

2. WIDEBAND TAPPED DELAY LINES

There are many applications for filters and correlators in radar signal processing, and these filters often take the form of tapped delay lines with specified (possibly variable) weights at each tap. The wideband capabilities of optical fibers, laser sources, and photodetectors make feasible the application of tapped delay-line filters to detection, identification, and pattern recognition utilizing wideband input data. For example, a tapped delay-line filter can be implemented, as shown in fig 19, with a fiber optics bundle consisting of fibers cut to predetermined lengths. Since the fiber diameter is small, the size of the bundle is not prohibitive; in addition, the tap spacings can be located very accurately.[33]

The detection of a target by a high-resolution radar can be enhanced by spatial matched filtering when the radial dimension of the target is large compared with the range resolution. For example, suppose the target is modeled as a set of point scatterers[46] located along the target's radial length. Then, the signal returned from a narrow pulse will vary according to the location and cross section of these scatterers. If a tapped delay line is implemented so that the delay between taps corresponds to the distance between scatterers and the attenuation (weight) at each tap corresponds to the scatterer cross section, then this "matched filter" will increase the SNR and thus enhance detection. For a radar having range resolution of 1 foot, the required tap-spacing accuracy easily can be met using several fibers cut to the appropriate lengths, or a single fiber tapped by reduction of cladding by etching.[33]

The technique mentioned above for enhancing detection can also be used for recognition and identification. For example, using a radar with high range resolution, the returns from objects of different shapes will produce different "signatures." These differences, if known or measured a priori, can be exploited to identify the particular target being detected, or to discriminate among types of targets. The identification procedure can be implemented using a tapped delay line (one for each type to be identified), with the tap weights determined by the shape of the object to be identified. For the broadband signals which are necessary for this application, fiber optics can provide the necessary bandwidth and tap-spacing capability.

Another application of fiber optic tapped delay lines is in a pulse compression network for broadband coded (eg, chirp or biphase) signals. These signals are used for the purpose of providing greater pulse energy while maintaining high range resolution, especially when the radar transmitter is peak-power limited. With the use of fiber optic tapped delay

---

[45]Schwartz, M, and Shaw, L, Signal Processing: Discrete Spectral Analysis, Detection, and Estimation, McGraw Hill, New York, 1975

[46]Rihaczek, AW, Principles of High-Resolution Radar, McGraw Hill, New York, 1969

lines, increased bandwidth can be used for (relatively) long-duration signals, thus allowing the use of large time-bandwidth signals.

As an example, consider the biphase modulated signal of the form

$$X(t) = \sum_{k=0}^{N-1} P_T(t-kT) \cos(\omega t + U_k \pi) \qquad 0 \leq t \leq NT,$$

where $P_T(t) = 1$ for $0 \leq t < T$, and where $U_0, U_1, \ldots, U_{N-1}$ is a specified sequence with $U_k = 0,1$. (The "code" sequence U_k is appropriately chosen so that the resulting signal has certain properties. Choice of "codes" is discussed in detail in Berkowitz[38] and Dixon,[39] for example.) The duration of the signal X(t) is NT; however, the inherent resolution properties of the signal are equivalent to a signal having duration T. If the received signal is multiplied by cos ωt (and low-pass filtered) the result is:

$$X_c(t) = \sum_{k=0}^{N-1} V_k P_T(t-kT)$$

where $V_k = 1 - 2U_k$ ($v_k = \pm 1$); ie, $X_c(t)$ is the envelope of X(t).

A pulse compression filter for $X_c(t)$ consists of an N-tap delay line with incremental delay T between taps. For small T (eg, 1–5 nanoseconds) and large N (1000 or greater), it is feasible to use a fiber optic delay line for the pulse compression filter. In most applications, two filters are required since the phase of X(t) is unknown. That is, the incoming signal X(t) is also multiplied by sin ωt to produce the quadrature component $X_s(t)$, and $X_s(t)$ is passed through a compression filter identical to the one for $X_c(t)$. The two filter outputs are combined to produce the desired output.

Another example is the generation and processing of nonlinear FM (chirp) signals. By using a group of optical fibers, each cut to appropriate lengths, a pulse compression filter for nonlinear FM pulse signals can be implemented. The input to the group of fibers is as shown in fig 19, and the tap spacing (ie, the fiber lengths) and attenuation are determined by the signal to be processed. By interchanging the roles of input and output (ie, the location of the photodetector and laser are interchanged) and applying an impulse, the output waveform for modulating the rf carrier can be generated. If variable-length delay lines are used and if the optical attenuators are also variable, the waveform used can be varied on a pulse-to-pulse basis. In addition, adaptive schemes for optimizing detection of particular targets can be applied by varying tap spacings and tap weights.

B. ELECTRONIC WARFARE

1. EW/ESM SIGNAL PROCESSING (SINGLE PLATFORM)

ESM signal processing has consisted largely of signal sorting by frequency and pulse repetition interval (PRI). Current and projected future emitters are becoming more exotic, the simplest "exotic" being PRI jitter or stagger, the next being minor frequency agility (less than 1%), followed by frequency hopping (5 to 15% frequency agility). Further complications are presented by frequency chirp signals and instantaneous spread spectrum (usually split-phase pseudorandom) signals. Consequently, it has been recognized that the only

parameter not under rapid control of the emitter is its physical location. Therefore, emphasis should be placed upon signal sorting techniques which rely on direction of arrival (DOA) or other effects which depend primarily upon spatial location. In addition, the historic trend of higher-power emitters (peak power and cw power) at ever higher frequencies will continue. The simultaneous presence of narrowband and broadband (hopping and spread spectrum) emitters presents conflicting requirements upon the design of ESM receivers. The acousto-optic Bragg cell is an attempt at resolving these conflicts. Potentially, the Bragg cell spectrum analyzer is envisioned as a channelized receiver. The readout techniques employed, however, reduce the available dynamic range to about 25 dB and also obliterate necessary signal parameters such as pulse time of arrival (for PRI determination), pulse group coding (if any), pulse width and pulse amplitude. The dynamic range is limited primarily by the fact that the CCD or photodiode readout arrays are optimized for high optical aperture efficiency (a close-packed array with very small spacings between elements). The high clock rates, used to read out the arrays rapidly, induce crosstalk and effectively raise the noise floor. The dynamic range could be improved substantially (to about 45 to 50 dB) by using a linear array of multi-mode light fibers to distribute the Bragg cell focal plane to several low-density readout arrays which are optimized for low crosstalk noise. Improvements in readout rate (currently a single large linear array of photodiodes or charge-coupled devices (CCDs) is used) by read-out array segmentation and technology improvement eventually may improve to the point at which crude pulse time of arrivals (TOAs) are available (±5 microseconds or so for single arrays to ±1/2 microsecond for the segmented fiber optic low-density readout array combination). It seems, however, that parameters such as pulse amplitude, pulse group coding, and pulse width will still remain unavailable.

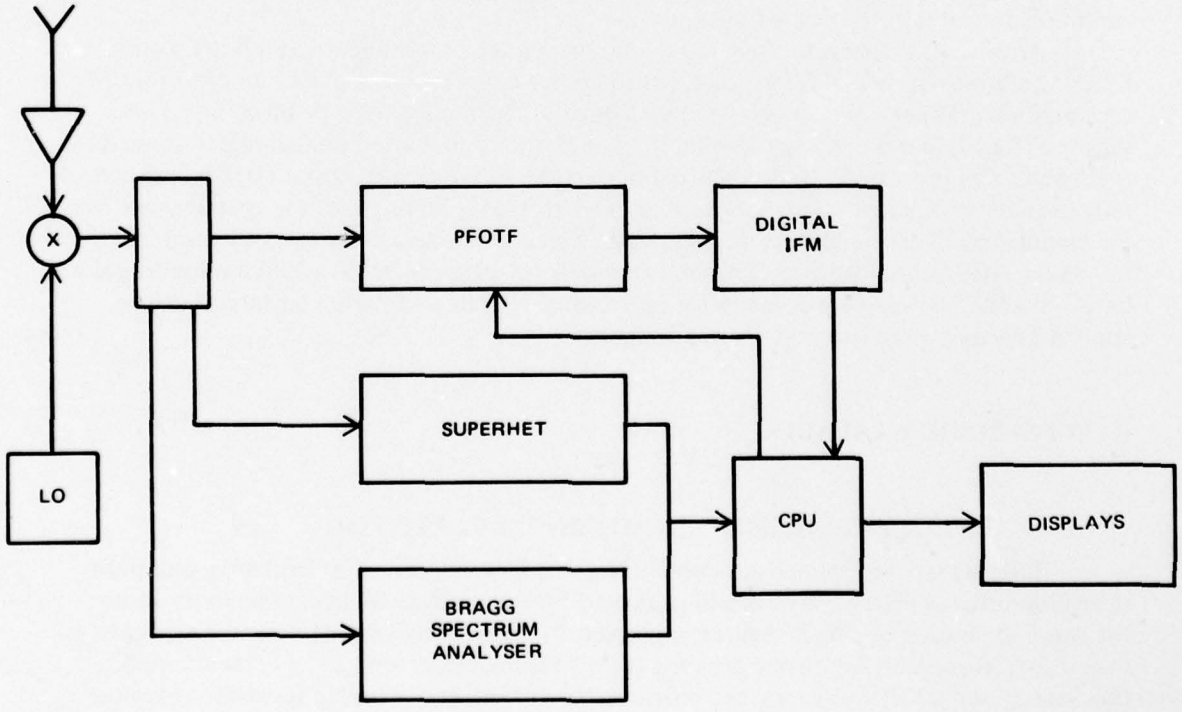

Figure 30. Hybrid adaptive ESM receiver.

A way of getting around the conflicting receiver requirements may be through the use of the programmable fiber optic transversal filter (PFOTF). Basically, the PFOTF consists of several high-bandwidth fibers illuminated by a single modulated light source. Each fiber is a different length, usually (but not necessarily) a fixed increment longer than the previous fiber. The output end of each fiber is passed through an electrically variable optical attenuator (ranging from integrated optical attenuators for the highest programming bandwidth to liquid crystal arrays used in either transmittance or reflectance modes for lower programming bandwidths). The outputs of all fibers are then summed (incoherently with respect to the light carrier) in a single photodetector. The PFOTF can be used to implement, on a dynamic basis, single or multiple bandpass and stop filters, matched filters, or "beamforming" in the matched filter domain to determine such things as chirp slope or chirp signals. The PFOTF could then be used to implement an adaptive IF filter in front of a hybrid superheterodyne and IFM receiver. This receiver could use the Bragg cell spectrum analyzer for priority search designation (see fig 30). A variation of the PFOTF, the variable-time increment transversal filter (see section III-B and fig 18) is an additional powerful tool for analysis of both linear and nonlinear chirp signals.

One problem which ESM receivers face is that all signal processing must be done on a one-pass basis; there is no second chance. The optical analog-to-digital converter operating at gigaword/s rates (see technology section for description) combined with long recirculating fiber optic delay-line memory loops can store broadband (300 to 500 MHz) signal data excerpts (1000 to 2000 microseconds) for indefinite periods of time (see fig 31). This would provide the capability to analyze repetitively a time slice of signal spectrum in an adaptive hypothesis testing manner. Airborne systems could use this technique for fine-grain pulse analysis and signature recognition.

An extension of the recirculating spectrum storage technique utilizing a two-channel receiver (see fig 32) could compute direction of arrival (DOA) on spread-spectrum signals utilizing cross correlation or convolution to derive time difference of arrival. This method has the advantage of substantial signal-to-noise improvement (because of signal autocorrelation) over leading-edge gating and carrier-frequency independence, as well as signal-to-noise improvement over interferometer techniques. This technique would be useful primarily with signals above 500 MHz, with bandwidths in excess of 100 MHz.

For frequencies between 100 and 500 MHz, the matched-delay filter is particularly useful for determining the angle of arrival of an incoming signal, as illustrated in fig 33. It is assumed that a plane-wave radar signal is incident at a certain angle θ to the axis of a linear array of antennas. The time delay τ_n between array element n and n + 1 is $\tau_n(\theta) = (\ell_n - \ell_{n+1}) \cos\theta/c$, where ℓ_n and ℓ_{n+1} refer to the positions of adjacent antennas and c is the velocity of light. The antenna signals will be denoted by $V_{sn}(t)$. These can be summed coherently by transmitting the n^{th} signal through a delay of length $\Upsilon_n(\theta_o)$ so that

$$V_o(t,\theta) = \sum_{n=1}^{N} V_{sn}[t - \tau_n(\theta_o)].$$

As θ varies, the filter output will have a peak for $\theta = \theta_o$. Separate filters designed for peak response at different angles $\theta_o(j)$, j = 1, ... ,M, can be provided to give an accurate indication of the arrival angle of one signal or simultaneously to monitor signals arriving at different angles. An important virtue of this technique is that the angular peak will be independent of frequency—thus permitting the creation of fixed multibeam DF arrays whose beam directions are independent of frequency.

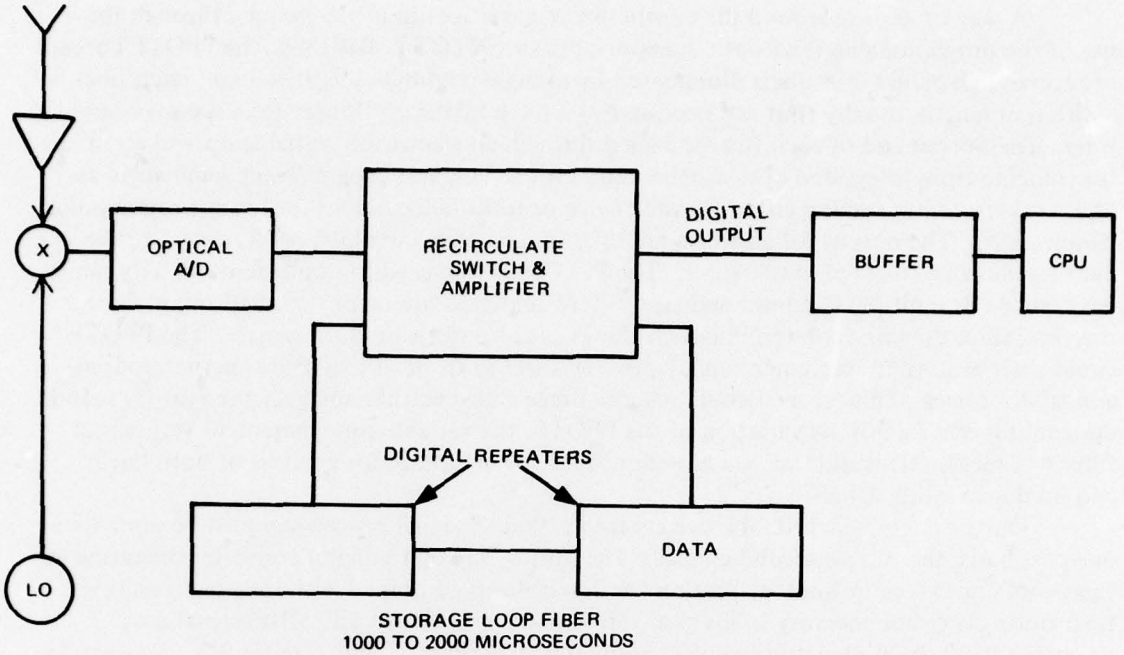

Figure 31. Recirculating loop fine-grain analysis ESM receiver.

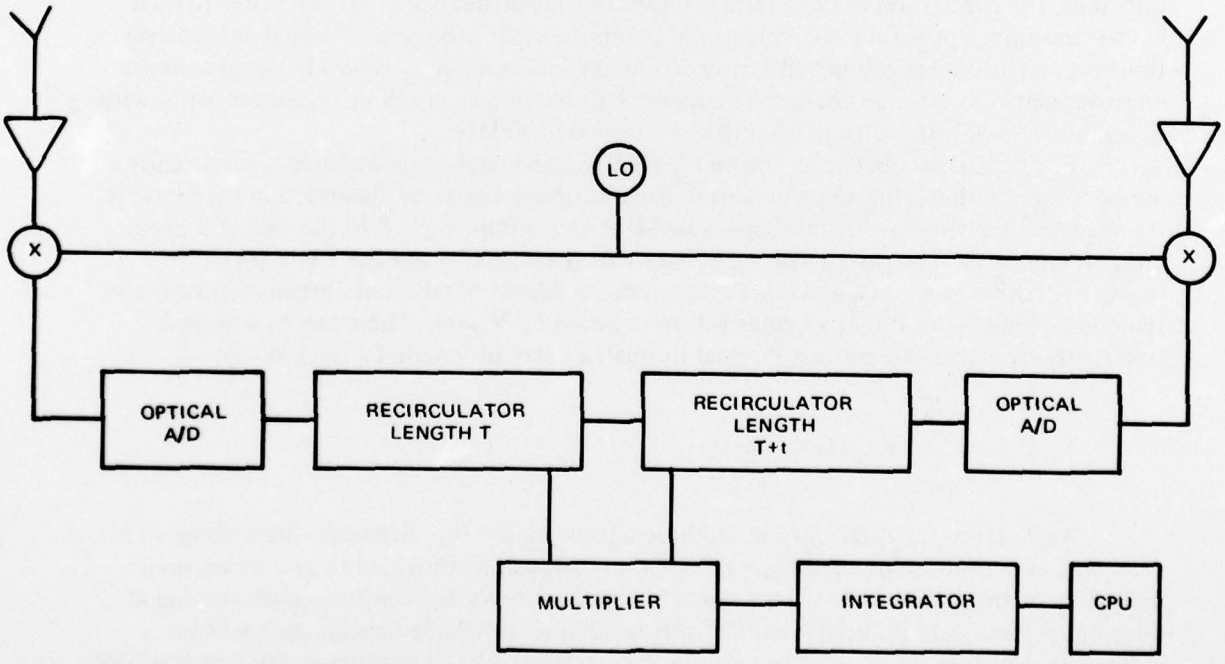

Figure 32. Time difference of arrival by broadband cross correlation.

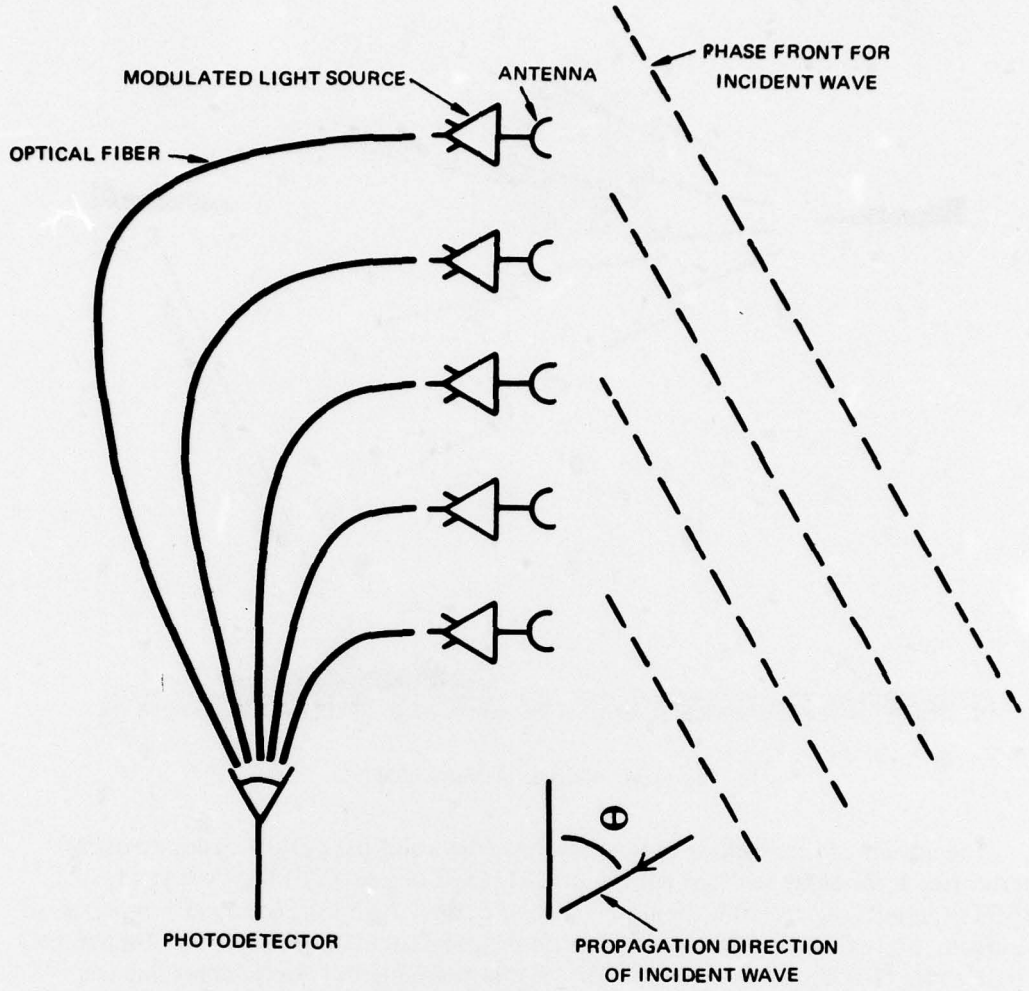

Figure 33. Fiber optics transversal filter for use in determining angle of arrival of incoming signal.

As the bandwidths of fibers and linear light source modulators increase, this technique will become applicable at higher frequencies, eventually up to 2 and 3 GHz.

2. MULTIPLATFORM ESM

The multiplatform role of real-time tactical ESM has been minor, primarily for two reasons: (1) lack of high-bandwidth direct ship-to-ship or ship-to-air dedicated ESM data links and (2) inability to store or process the broadband data required. With the rapid advance of millimetre wave components, broadband (approximately 500 MHz), short-range (about 20 nautical miles), highly directional data links are now feasible. If these links utilized highly directional low-sidelobe antennas and were operated at an atmospheric absorption frequency, they would be usable in all but the most stringent EMCON conditions and heavy rainfall. For fair-weather operations at somewhat shorter ranges but superior EMCON effectiveness, cw CO_2 lasers could be used (see fig 34).

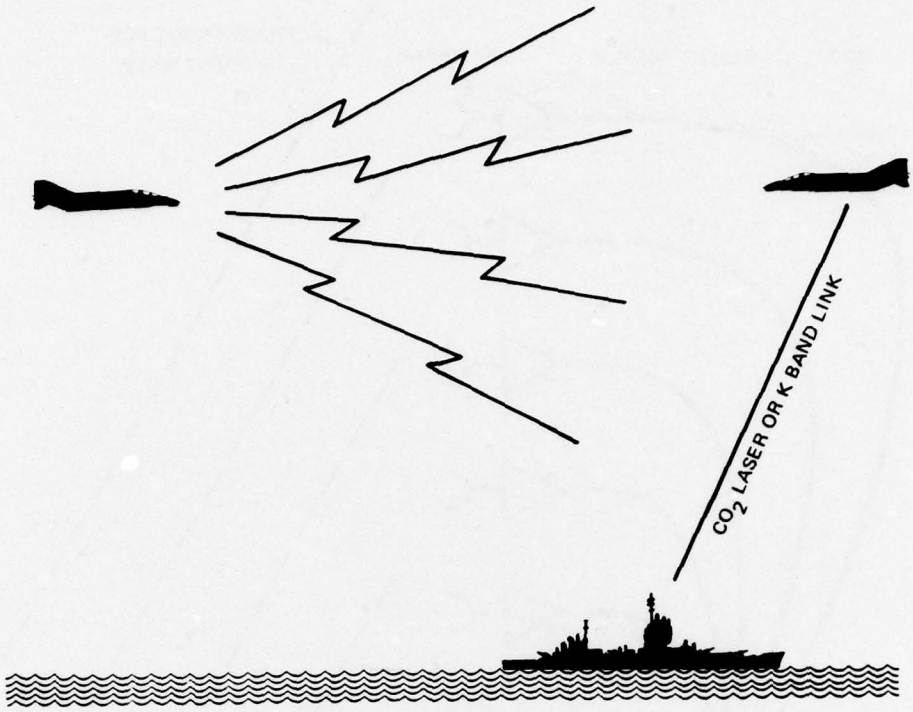

Figure 34. Multiple platform ESM.

The advent of single-mode optical low-loss fibers and the optical analog-to-digital converter (see technology section) with multi GHz logic devices (TELDs, OATs and MESFETs) permits recirculating memories with extremely high time bandwidth products to be achieved. For example, a 1000-microsecond memory circulating 8-bit words (in parallel) at a 1-GHz rate (1 million 8-bit words). The digitally variable fiber optic delay line (see technology section), when combined with the recirculating memories and ship-to-ship data links, could provide impressive ESM signal-processing capabilities, such as complex pulse-train deinterleaving irrespective of PRI irregularities and frequency hopping, direction finding (frequency independent), and passive ranging. The basic pulse-train deinterleaving would be accomplished by using the digitally variable delay line to slide, in time, the raw ESM data from one platform past the data from another until the two pulse trains match in time (the decision criterion being based upon the probability of N matches out of M pulses for K random pulse trains); see fig 35. To reduce the search time, additional fiber optic delay lines, each incrementally longer than the previous one, could be used simultaneously to match relatively large time slices with high time resolution. For example, 100 to 1000 fibers with 50-nanosecond length differences could be used to search time shift slots for 5 to 50 microseconds. This technique would be adequate for emitters of any PRI type as well as pulsed frequency hoppers, provided that the minimum PRI interval is greater than the time difference separation of the two ships. Radar emitters which have PRIs shorter than the time delay difference between the two ships (less than 120 microseconds) must have some other modulation scheme (such as pulsed doppler) for their own ranging function. The time shift ambiguity could then be resolved by determining the offset of the secondary modulation envelopes. Rapid frequency chirp emitters (chirp times less than 10 microseconds or so)

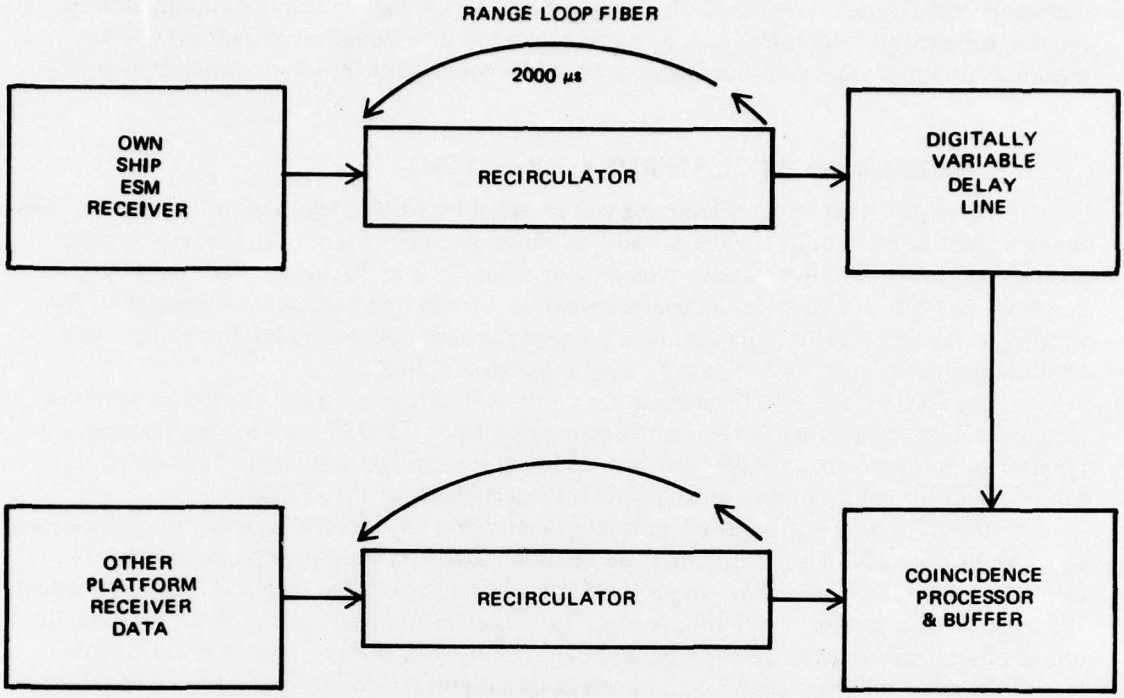

Figure 35. Multiple-platform time-shift pulse-train deinterleaver.

simply could be treated as pulses and the same methods could be applied. Exotic instantaneous spread spectrum would require a finer time search using a 100 to 1000 delay sum fiber array with tap spacings of 1 nanosecond or so.

If one assumes a low to moderate elevation angle (less than 30 degrees) for the emitter, with the time differences derived for each ship's measurement of the emitter and an angle to the emitter from one ship, then passive range to the emitter can be determined (with better accuracy than two-point angular triangulation). If the emitter is scanning in some discernible fashion (circular, sector, conical, etc), the range uncertainty can be reduced by using the scan angular rate and the time offset between the two ships (in effect, one computes the angular difference between the two ships as seen by the emitter). With three ships participating, the moderate elevation geometry position DF and range can be computed from just the time differences.

These improved multiship ESM capabilities would greatly enhance long-range targeting in a jamming environment and provide valuable correlation data for radar intercepts and tactical scenario determination (ARM threat determination and multiship counter ARM tactics).

One additional feature of the ESM data link would be to provide own-force emissions blanking.

3. ELINT

An increasingly difficult area of ELINT, that of predetection recording of broad bandwidth signals, could be aided by integrated optics. The integrated optical analog-to-digital

converter with a laterally scanned film recorder (see technology section) could be used to provide broadband (500 MHz) high dynamic range (48 dB) digital recordings of 3 to 6 minutes' duration. The recording format would be convenient for later computer analysis.

4. ELECTRONICS COUNTERMEASURES (ECM)

Three potential areas of jamming can be aided by fiber/integrated optics devices. The first is repeat backjamming for the purpose of range-gate deception. The digitally variable analog fiber optic delay line would provide long delays (10 to 30 microseconds) and broadband signals (200 to 300 MHz) in fine increments (5 to 20 nanoseconds). Admittedly, this technique would be useful only against a relatively unsophisticated radar, but it does provide additional security by providing a very large range gate pulloff.

The second area is in the generation of complex broadband waveforms for jamming purposes. The programmable fiber optic transversal filter (PFOTF) can be used to generate highly complex broadband wave forms from simple sets of light impulses. The waveforms can be changed rapidly simply by changing the coefficients of the PFOTF.

The third area is primarily applicable to jamming of spread spectrum communications or navigation signals. Two techniques can be used. The first simply employs a set of different-length fiber delay lines to produce delayed replicas of the signal, thereby presenting the receiver with several correlation peaks. If the correlation peaks are sufficiently close to one another, one broad correlation peak should result, with the subsequent result of data loss to the receiver. The second communications jamming technique would use a PFOTF to store a segment of the signal and then retransmit it in reverse order. This would reduce the signal gain in the receiver and make the receiver more susceptible to conventional noise jamming.

C. COMMUNICATIONS

Many of the signal-processing techniques required in communication systems can be implemented with fiber and integrated optic devices. Communication rates (in data bits per second) have increased considerably in recent years, and more attention is being given to low-probability-of-intercept (LPI), antijam (AJ), and secure systems. Therefore, the time-bandwidth product necessary for communication signals has become very large. This means that processing techniques applicable to large time-bandwidth signals must be used, and fiber and integrated optic devices can perform many of the required high-speed operations, such as correlation, filtering, etc.

An important component of an LPI, AJ, or secure communication system is a means for generating a pseudorandom code. In an LPI or AJ system, this code is used to determine, at the transmitter, how the signal energy will be distributed in time and frequency. The receiver then uses the same code to "strip off" the time/frequency modulation so that the data bits can be determined. For a secure system, a code is used at the transmitter to "scramble" the input data to remove intelligibility. The receiver then applies the same code to unscramble the data.

Codes for AJ (or LPI) and security can be applied in the same system; however, they are, in general, generated independently and with different properties. For example, codes for AJ must have extremely low cross-correlation and unambiguous autocorrelation properties (Dixon[40], page 65), while codes used for security must present an unintended party with great difficulty in decipherability.

Since the data rate for communication can be several megabits per second, the code rates must be much higher so that reasonable time-bandwidth products or message security can be achieved. This means that code rates of hundreds of megachips per second are necessary. (To distinguish code "bits" from data bits, the code elements are referred to as "chips" (see ref 40).) The pseudorandom sequence generator described in a previous section can provide a means for generating and combining codes at chip rates approaching gigachips per second. Also, by utilizing the variable-length delay lines achievable by means of fiber optics and optical switches, codes applicable to message security can be generated at high rates.

D. MULTISENSOR CORRELATION PROCESSING

Multisensor correlation processing presently is done by special-purpose digital computers. In some cases the required computation rates exceed by several orders of magnitude the capacity of present central processing units. One possible solution to the problem is to utilize a large number of high-speed central processors operating in parallel. A switch would be needed in such a system to route data between these central processors and buffers and memories. If the data rates are high (> 200 Mb/s), integrated optics seem to provide the only practical approach to implementation of such a switch. A system utilizing such a switch is illustrated schematically in fig 36.

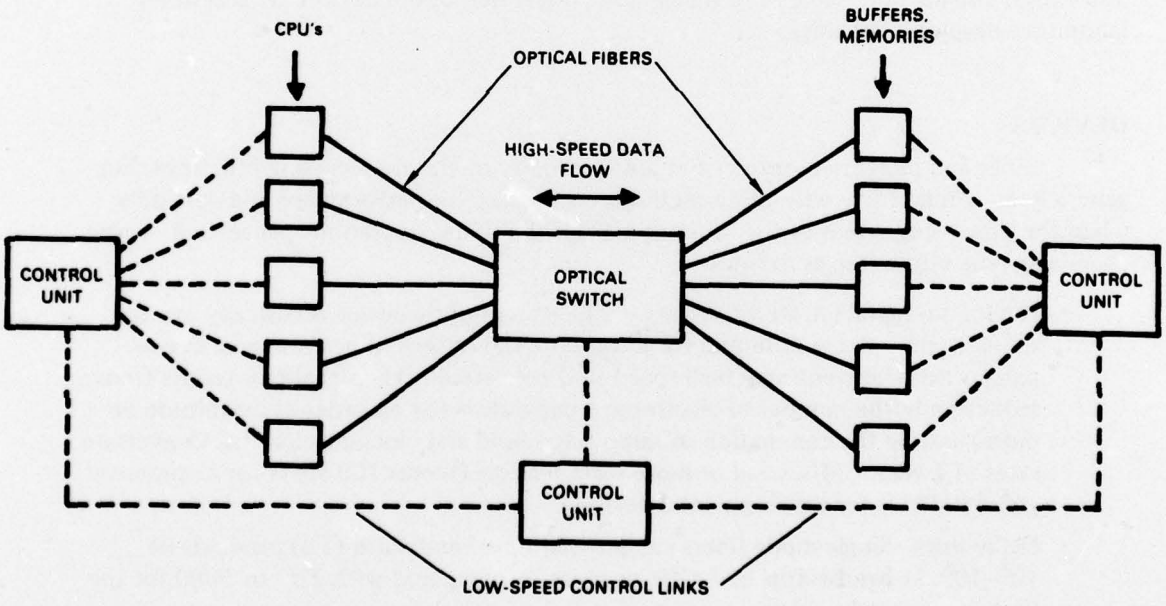

Figure 36. System for high-speed parallel computation utilizing an integrated optical switch.

V. CONCLUSIONS

BASIC TECHNOLOGY

The technologies of fiber optics and integrated optics have advanced rapidly during the past few years. Some recent developments representative of the present state of the art are as follows:

- Fibers with a loss of 0.5 dB/km (see ref 6)
- Injection lasers operating continuously at room temperature for over 10 000 hours
- An optical repeater which operates at 800 Mb/s with 40-dB optical gain[47]
- An optical modulator-switch with 1-ns response[16]
- A 2 X 2 optical switch with 26-dB channel isolation,[20] and a 4 X 4 switching network[48]
- Permanent coupling between single-mode fibers with 1-dB loss[10] and demountable coupling between single-mode fibers with 0.5-dB loss.

Low-loss multimode fibers are in large-scale production for the telecommunications industry, and manufacturing capability for transmitters, receivers, and connectors for use with fibers also exists. Single-mode fibers and single-mode integrated optics devices are still in the laboratory development stage.

DEVICES

Fiber and integrated optics offer a wide variety of signal-processing functions, but generally are competitive with other methods on the basis of performance and cost only when the processing rate is of the order of 10^8 (100 million) operations per second. Some promising possibilities are as follows:

- Analog-to-digital (A/D) converters – The electro-optic device is basically much simpler and has the potential for lower cost and improved performance in comparison with conventional high-speed A/D converters. The simplicity results from a reduction in the number of electronic comparators (by an order of magnitude or more) and by the elimination of sample-and-hold and clocking circuits. Conversion rates of 1 gigaword/second or more seem feasible (versus 100 Mw/s for commercial and 400 Mw/s for developmental devices).
- Delay lines–Single-mode fibers can provide time-bandwidth (TB) products of 10^5–10^6, at bandwidths of 1 GHz or more, as compared with TB's of 5000 for the best acoustic delay lines.
- Transversal filters–The fiber optics transversal filter has the potential for processing of wideband (> 1 GHz) signals, with rapid (10 ns) programmability of tap weights and spacings. This represents a new capability not available with other techniques

---

[47] Nawata, K, and Takano, K, "800 Mb/s Optical Repeater Experiment," Electron Lett, v 12, p 178-180, April 1976

[48] Schmidt, RV, and Buhl, LL, "Experimental Optical 4 X 4 Switching Network," Electron Lett, v 12, October 1976

for constructing adaptive filters and waveform generators. Fiber transversal filters also would make it possible to have a large number (> 500) of taps, with precise (< 100 ps) tap spacings, and the sensitivity to temperature variations is less than for surface acoustic wave filters.

- Pseudorandom sequence generators – The optical sequence generator is much simpler than its electronic counterpart, and is capable of at least a factor of five in speed (1 Gb/s versus 200 Mb/s) and substantial increase in sequence length.
- Bragg cell spectrum analyzers – An integrated optics device has the potential to reduce electrical drive power requirements by a factor of 10 dB or more in comparison with the bulk device, provided that it can be fabricated in TeO_2 or a comparable material. The bulk device will probably retain an advantage of about a factor of 2 in bandwidth, because the bulk transducer has an inherently greater bandwidth than the surface-wave transducer used in the integrated optics device.
- Switching network – It is feasible to integrate 1000 or more optical 2 X 2 switches on a single substrate. It appears that it is possible to implement a large (>20 X 20) switching network with data rates in excess of 1 Gb/s and fast (10–100 μs) reconfiguration rate. Electronic switches are limited to data rates less than 250 Mb/s and to only a very few terminals at that data rate.

RADAR APPLICATIONS

There are several signal-processing functions required by radar systems which can be implemented using fiber and integrated optics components. These signal-processing functions include matched filtering, pulse-to-pulse integration, and the generation and processing of wideband signals.

- In the case of pulse-to-pulse integration, when the signal bandwidth exceeds 500 MHz and the interpulse period is larger than 200 μs, fiber optic delay lines provide the only reasonable storage medium, if the signal bandwidth is to be preserved. Emitter-coupled logic (ECL) shift registers could approach the bandwidth requirement; however, for simple binary quantization (1 bit), approximately 10^4 shift-register stages would be required to store all of the (binary) data from a single transmitted pulse.
- For matched filtering: the use of fiber optic tapped delay lines can provide capabilities not easily achievable using other techniques, such as identifying (or classifying) targets based on high-resolution radar "signatures." These tapped delay lines can require tap spacings as small as a few nanoseconds, and as many as several hundred taps. Also, the bandwidth required can be as high as 500 MHz, and this bandwidth is required at all taps. Therefore, it appears that by implementing matched filters with fiber optic delay lines, performance not achievable by any other means can be achieved.
- The generation and processing of wideband signals can also be achieved using fiber optic delay lines. If the lengths of the individual fibers making up the tapped delay line are also made variable (as discussed earlier, see fig 18), a very flexible and broadband adaptive signal generator/processor can be implemented. An example is the generation and processing of nonlinear frequency-modulated radar signals such that the frequency modulation is varied from pulse to pulse or is adapted to the detection of a particular set of targets.

ELECTRONIC WARFARE APPLICATIONS

The programmable fiber optics transversal filter (PFOTF) represents a powerful tool for both signal analysis and sorting in ESM, and the generation of complex broadband waveforms for active EW. Such a versatile device could implement, on a dynamic basis, single or multiple bandpass or bandstop filters, and matched filters for sorting on the basis of frequency, chirp slope, and other signal characteristics. It could also be used as an adaptive IF filter in front of a hybrid superheterodyne or IFM receiver (see fig 30). For active EW, the PFTOF could be used to generate complex, agile jamming waveforms with bandwidths of several hundred megahertz to 1 gigahertz.

Delay-matched fiber optics filters would also provide new capability for determining the direction of arrival (DOA) of one or more incoming rf signals in the vhf and uhf bands with an array of omnidirectional antennas (see fig 33). The fiber optics device has the advantage that, unlike electronic phased interferometers, it is not frequency dispersive. With present components, the technique is most useful for signal frequencies in the 100–500-MHz range, but performance in the 2–3-GHz band can be expected within 3–5 years using improved components.

The signal storage capacities of very long optical fiber recirculating memories combined with the high-speed optical analog-to-digital converter create the possibility of new techniques that will permit multiple-platform, medium-range ESM surveillance with high accuracy, passive ranging, and position fixing capabilities (fig 34 and 35). These same techniques may find use in Marine Corps or Army applications.

The optical analog-to-digital converter offers a relatively inexpensive means of recording broadband (500 MHz) signals for ELINT purposes.

The Bragg cell is proving to be a device of significant interest to the EW community, because it is capable of instantaneous broadband spectral analysis. However, there are a number of drawbacks and limitations in using Bragg techniques which should not be minimized. Chief among these are readout rate limitations which will limit the knowledge of pulse time of arrival (TOA) to ±5 microseconds for single readout arrays or ±1 microsecond for segmented arrays, at best. Therefore, only crude PRI sorting will be possible, with no pulse group or pulsewidth information available. These deficiencies can be offset by augmenting the Bragg analyzer with certain fiber optics and integrated optics devices like the programmable fiber optics transversal filter, the high-speed optical A/D converter, and recirculating memories for signal storage and analysis in very long fiber delay lines. The hybrid adaptive ESM receiver (shown in fig 30) is a good example of this.

COMMUNICATIONS APPLICATIONS

The pseudorandom sequence generator using fiber optics and integrated optics, which offers the possibility of generating and combining long sequences ($2^{50}-1$) to ($2^{100}-1$) at gigachip rates, could lead to substantial improvements in data rates, probability of intercept, or immunity from jamming in spread spectrum systems. By using variable-length delay lines (fig 18), codes applicable to message security can be generated at high rates.

MULTISENSOR CORRELATION APPLICATIONS

An integrated optics switch, used in conjunction with electronic central processing units, buffers, and memories, offers the possibility of substantial improvement in computation speed for multisensor correlation problems.

VI. RECOMMENDATIONS

1. Implement an eight-beam feasibility test model of the fiber optic beam-forming antenna for ESM direction finding in the vhf/uhf band and determine the sensitivity, dynamic range, and angular accuracy.

2. Develop an 8-bit optical A/D converter operating at 1 gigaword/second with a fiber loop for recirculating data storage.

3. Use the A/D converter described in paragraph 2 to demonstrate the feasibility of signal analysis for exotic ESM waveforms and monopulse imaging for high-resolution radar.

4. Perform feasibility study, operational analysis, and cost-benefit projections of multiple-platform ESM techniques that could be implemented with dedicated low-power data links and the use of fiber optics and integrated optics devices.

5. Develop a 1-gigabit/second optical pseudorandom sequence generator for spread-spectrum communications.

6. Develop a fiber optics recursive filter for demonstrating feasibility of pulse-to-pulse integration in high-resolution radars.

7. Investigate the effectiveness of tailored waveform generation using a programmable fiber optics transversal filter (PFOTF) for jamming and deception purposes. If warranted by the results of the investigation, develop such a waveform generator.

8. Perform systems analysis and computer simulation of hybrid Bragg cell-PFOTF superheterodyne and IFM receivers and determine if projected capabilities warrant development of such a system and associated components.

9. Demonstrate the feasibility of Bragg cell dynamic range improvement using fiber optics techniques.

REFERENCES

1. Tamir, T, ed, Integrated Optics, Springer Verlag, Berlin, 1975
2. Kogelnik, H, "An Introduction to Integrated Optics," IEEE Trans Microwave Theory and Techniques, v MTT-23, p 2-16, January 1975
3. Taylor, HF and Yariv, A, "Guided Wave Optics," Proc. IEEE, v 62, p 1044-1060, August 1974
4. Personick, SD, "Optical Fibers, a New Transmission Medium," Communications Society, v 13, p 20-24, January 1975
5. Miller, SE, Maractili, EAJ, and Li, T, "Research Toward Optical Fiber Transmission Systems," Proc IEEE, v 61, p 1703-1751, December 1973
6. Horiguchi, M, and Osanai, H, "Spectral Losses of Low-OH-Content Optical Fibers," Electron Lett, v 12, p 310-312, 10 June 1976
7. Lee, TP, and Cho, AY, "Single-Transverse-Mode Injection Lasers with Embedded Stripe Laser Grown by Molecular Beam Epitaxy," Appl Phys Lett, v 29, p 164-166, 1 August 1976
8. Blum, J, McGroddy, JC, McMullin, PG, Shih, KK, Smith, AW, and Ziegler, JF, "Oxygen-implanted Double-Heterojunction GaAs/GaAlAs Injection Lasers," IEEE J Quant Electron, v QE-11, p 413-418, July 1975
9. Lee, TP, Burrus, CA, Miller, BI, and Logan, RA, "$Al_xGal\text{-}xAs$ Double-Heterostructure Rib-Waveguide Injection Laser," IEEE J Quant Electron, v QE-11, p 432-435, July 1975
10. Pavlopoulos, TG, private communication
11. DiDimenico, M, "A Review of Fiber Optical Transmission Systems," Optical Engineering, v 13, p 423-428, September-October 1974
12. Kuhn, L, Dakss, ML, Heidrich, PF, and Scott, BA, "Deflection of an Optical Guided Wave by a Surface Acoustic Wave," Appl Phys Lett, v 17, p 265-267, September 15 1970
13. Tsai, CS, Alhaider, MA, Nguyen, LT, and Kim, B, "Wide-band Guided-Wave Acousto-optic Bragg Diffraction and Devices Using Multiple Tilted Surface Acoustic Waves," Proc IEEE, v 64, p 318-327, March 1976
14. Kaminow, IP, "Optical Waveguide Modulators," IEEE Trans Microwave Theory and Tech, v MTT-23, p 57-70, January 1975
15. Kaminow, IP, and Turner, EH, "Electro-optic Light Modulators," Proc IEEE, v 54, p 1374-1390, October 1966
16. Martin, WE, "A New Waveguide Switch/Modulator for Integrated Optics," Appl Phys Lett, v 26, p 562-564, May 1975
17. Ohmachi, Y, and Noda, J, "Electro-optic Light Modulator With Balanced Bridge Waveguide," Appl Phys Lett, v 27, p 544-546, November 1975

18. Campbell, JC, Blum, FA, Shaw, DW, and Lawley, KL, Appl Phys Lett, v 27, p 202–205, August 15 1975

19. Papuchon, M, Combewale, V, Mathieu, X, Ostrowsky, DB, Reiber, L, Roy, AM, Sejourne, B, and Werner, M, "Electrically Switched Optical Directional Coupler – Cobra," Appl Phys Lett, V 27, p 289–91, September 1 1975

20. Kogelnik, A, and Schmidt, RV, "Switched Directional Couplers with Alternating $\Delta\beta$," IEEE J Quant Electron, v QE-12, p 396–401, July 1976

21. Tasker, GW, and French, WG, "Low-loss Optical Waveguides With Pure Fused SiO_2 Cores," Proc IEEE, v 62, p 1281–1282, September 1974

22. Snitzer, E, "Cylindrical Dielectric Waveguide Modes," J Opt Soc Amer, v 51, p 491–498, May 1961

23. Jurgensen, K, "Dispersion-Optionized Optical Single Mode Glass Fiber Waveguides," Appl Opt, v 14, p 163–168,

24. Hoeschele, DF, Jr, Analog-to-Digital/Digital-to-Analog Conversion Techniques, New York, Wiley, 1968

25. Sheingold, DH, and Ferrero, RA, "Understanding A/D and D/A Converters," IEEE Spectrum, v 9, no 9, p 47–56, September 1972

26. Taylor, HF, "An Electro-optic Analog-to-Digital Converter," Proc IEEE, v 63, p 1524–1525, October 1975

27. Denton, RT, Chen, FS, and Ballman, AA, "Lithium Tantalate Light Modulators," J Appl Phys, v 38, p 1611–1617, March 15, 1967

28. Zernike, F, "Integrated Optics Switch," presented at the OSA/IEEE Topical Meeting on Integrated Optics, New Orleans, La, June 1974

29. Rimmel, AW, "State-of-the-Art Analog-to-Digital Conversion Equipment," Report R-4657, Battelle Columbus Laboratories, Columbus, Ohio, April 1975

30. Wright, S, Mason, IM, and Wilson, MGF, "High-Speed Electro-optic Analog-to-Digital Conversion," Electron Lett v 28, p 508–509, November 28, 1974

31. Paoli, TL and Ripper, JE, "Optical Pulses from cw GaAs Injection Lasers," Appl Phys Lett, v 15, p 105–107, August 1, 1969

32. Taylor, HF, Martin, WE, and Caton, WM, "Channel Waveguide Electro-optic Devices for Communications and Signal Processing," presented at the IEEE/OSA Topical Meeting on Integrated Optics, Salt Lake City, January 1976

33. Wilner, K, and van den Heuvel, AP, "Fiber Optic Delay Lines for Microwave Signal Processing," Proc IEEE, v 64, p 805–807, May 1976

34. Dillard, GM, Taylor, HF, and Hunt, BR, "Fiber and Integrated Optics Techniques for Radar and Communications Signal Processing," National Telecommunications Conference Record, v III, p 37.5-1 to 37.5-5, December 1976

35. Slobodnik, AJ, Jr, "Surface Acoustic Waves and SAW Materials," Proc IEEE, v 64, p 581, May 1976

36. Darby, BJ, "Key Signal Processing Functions Performed with Surface Acoustic Wave Devices," Wave Electronics, v 2, p 266–290, July 1976

37. Slobodnik, AJ, "A Review of Material Tradeoffs in the Design of Acoustic Surface Wave Devices at VHF and Microwave Frequencies," IEEE Trans Sonics and Ultrasonics, v SU-20, p 315–323, October 1973

38. Wray, JH, and Neu, JT, "Refractive Index of Several Glasses as a Function of Wavelength and Temperature," J Opt Soc Amer, v 59, p 774–776, June 1969

39. Berkowitz, RS, Modern Radar, Wiley, New York, 1965

40. Dixon, RC, Spread Spectrum Systems, Wiley, New York, 1976

41. Taylor, HF, "Optical Waveguide Connecting Networks," Electron Lett, v 10, p 41–43, February 28, 1974

42. Soref, RA, "Optical Switch Study," TR 75-3, Rome Air Development Center, Rome, N. Y., February 1975

43. Benes, VE, Mathematical Theory of Connecting Networks, Academic Press, New York, 1965

44. Joel, AL, "On Permutation Switching Networks," Bell Syst Tech J, v 47, p 813–822, May-June 1968

45. Schwartz, M, and Shaw, L, Signal Processing: Discrete Spectral Analysis, Detection, and Estimation, McGraw Hill, New York, 1975

46. Rihaczek, AW, Principles of High-Resolution Radar, McGraw Hill, New York, 1969

47. Nawata, K, and Takano, K, "800 Mb/s Optical Repeater Experiment," Electron Lett, v 12, p 178–180, April 1976

48. Schmidt, RV, and Buhl, LL, "Experimental Optical 4×4 Switching Network," Electron Lett, v 12, Oct 1976